



An evolutionary paradox on threadsnakes: Phenotypic and molecular evidence reveal a new and remarkably polymorphic species of *Siagonodon* (Serpentes: Leptotyphlopidae: Epictinae) from Amazonia

Angele Martins^{1,2}, Manuella Folly², Guilherme Nunes Ferreira³, Antônio Samuel Garcia da Silva⁴, Claudia Koch⁵, Antoine Fouquet⁶, Alessandra Machado⁷, Ricardo Tadeu Lopes⁷, Roberta Pinto⁸, Miguel Trefaut Rodrigues⁹, Paulo Passos²

1 Departamento de Ciências Fisiológicas, Universidade de Brasília, Campus Darcy Ribeiro, Brasília, Distrito Federal, Brazil

2 Departamento de Vertebrados, Museu Nacional, Universidade Federal do Rio de Janeiro, Quinta da Boa Vista, Rio de Janeiro, Brazil

3 Programa de Pós-graduação em Biodiversidade, Universidade Federal do Oeste do Pará, Pará, Brazil

4 Averde Soluções Ambientais, Goiânia, Goiás, Brazil

5 Leibniz Institute for the Analysis of Biodiversity Change (LIB), Museum Alexander Koenig, Adenauerallee 160, 53113 Bonn, Germany

6 Laboratoire Evolution et Diversité Biologique (EDB), UMR5174, Bâtiment 4R1, 118 Route de Narbonne 31077, Toulouse, France

7 Instituto Alberto Luiz Coimbra de Pós-Graduação e Pesquisa em Engenharia, Laboratório de Instrumentação Nuclear, Universidade Federal do Rio de Janeiro, Rio de Janeiro, Rio de Janeiro, Brazil

8 Laboratório de Diversidade de Anfíbios e Répteis, Museu de Arqueologia e Ciências Naturais da Universidade Católica de Pernambuco, Recife, Brazil

9 Universidade de São Paulo, Instituto de Biociências, Departamento de Zoologia, Caixa Postal 11.461, CEP 05508-090, São Paulo, SP, Brazil

<https://zoobank.org/1228F910-CF16-4A6F-8706-FFD41E0C06E0>

Corresponding author: Angele Martins (amartins@unb.br)

Academic editor Uwe Fritz | Received 29 November 2022 | Accepted 16 March 2023 | Published 10 April 2023

Citation: Martins A, Folly M, Ferreira GN, Garcia da Silva AS, Koch C, Fouquet A, Machado A, Lopes RT, Pinto R, Rodrigues MT, Passos P (2023) An evolutionary paradox on threadsnakes: Phenotypic and molecular evidence reveal a new and remarkably polymorphic species of *Siagonodon* (Serpentes: Leptotyphlopidae: Epictinae) from Amazonia. *Vertebrate Zoology* 73 345–366. <https://doi.org/10.3897/vz.73.e98170>

Abstract

Threadsnakes are known for their conserved external morphology and historically controversial systematics, challenging taxonomic, biogeographic and evolutionary researches in these fields. Recent morphological studies—mostly based on μ CT data of the skull and lower jaw—have resolved systematic issues within the group, for instance leading to the description of new taxa or re-positioning little-known scolecophidian taxa in the tree of life. Herein we describe a new polymorphic species of the genus *Siagonodon* from Amazonia based on morphological (external, osteology and hemipenis) and molecular data, and provide the first hemipenial description for the genus. We also reassign *Siagonodon acutirostris* to the genus *Trilepida* based on osteological data in combination with molecular evidence. The new species described represents an evolutionary paradox for scolecophidians because the species displays a remarkable variation in the shape of the snout region that is otherwise always highly conserved in this clade. Finally, this study reinforces the importance of protected areas as essential in maintaining vertebrate populations, including those that are not yet formally described.

Keywords

Hemipenial morphology, intraspecific variation, Neotropics, osteology, phylogeny, polymorphism, Squamata

Introduction

The fossorial snakes known as ‘Scolophidia’ Cope, 1864 are divided in three major lineages—Anomalepididae Taylor, 1939, Leptotyphlopidae Stejneger, 1892, and Typhlopoidea Romer, 1945—altogether comprising about 460 species that occur throughout the globe, except for Antarctica (Vidal et al. 2010; Miralles et al. 2018; Uetz et al. 2022). These snakes have long posed challenges for researchers interested in elucidating their taxonomy, systematics, and consequently biogeography and evolution (Bell et al. 2021). However, recent contributions—most of them boosted by the use of high resolution digital images (Rieppel et al. 2009; Santos and Reis 2018, 2019; Koch et al. 2019; Martins et al. 2019a; Koch et al. 2021; Lira and Martins 2021; Laver et al. 2021; Deolindo et al. 2021; Martins et al. 2021a, 2021b)—have repeatedly highlighted morphological data (mostly osteological) as fundamental for elucidating longstanding unresolved or disputed issues in the literature (see Miralles et al. 2018). For instance, several studies (e.g., Koch et al. 2019, 2021; Martins et al. 2019a) have taken advantage of μ CT data to overcome the challenges imposed by the overall highly conserved external morphology of scolophidians, demonstrating the informativeness of skull and lower jaw characters for systematic studies (Laver and Daza 2021). The integration of these osteological data with molecular evidence has been particularly enlightening for taxonomically challenging clades (Graboski et al. 2018, 2022; Martins et al. 2019a).

The threadsnakes of the family Leptotyphlopidae currently comprise about 140 species that inhabit the Americas, sub-Saharan Africa, the Arabian peninsula and southwestern Asia (Adalsteinsson et al. 2009; Uetz et al. 2022). The subfamily Epictinae contains about 90 species allocated in ten currently recognized genera (Uetz et al. 2022; Martins et al. 2019a) that occur in the New World (Americas and Antilles: *Epictia* Gray, 1845; *Habrophallos* Martins et al., 2019; *Rena* Baird & Girard, 1853; *Mitophis* Hedges, Adalsteinsson & Branch, 2009; *Siagonodon* Peters, 1881; *Tetracheilostoma* Jan, 1861; and *Trilepida* Hedges, 2011) and in Africa (*Rhinoleptus* Orejas-Miranda, Roux-Estève & Guibé, 1970; *Rhinoguinea* Trape, 2014; and *Tricheilostoma* Jan, 1860). Adalsteinsson et al. (2009) proposed several changes to the leptotyphlopoid classification through molecular phylogeny in combination with literature data, mainly based on the external morphology (i.e., coloration, pholidosis and morphometrics). However, in many instances, there was no compelling phenotypic evidence from the internal morphological systems (e.g., bones, muscles, glands, viscera, genitalia) for taxa recognition, and the monophyly of some recognized genera have not been tested (e.g., *Siagonodon* and *Tricheilostoma* = *Trilepida*, sensu Hedges 2011; see below).

The genus *Siagonodon* currently comprises four species—*S. acutirostris* Pinto and Curcio, 2011, *S. borrichianus* (Degerbøl 1923), *S. cupinensis* (Bailey and Carvalho 1946), and *S. septemstriatus* (Schneider 1801)—that oc-

cur along the cis-Andean region of South America from northern French Guiana and Suriname, to its southernmost record in Argentina (Francisco et al. 2018). The genus was erected by Peters (1881) to accommodate *Anguis septemstriatus* Schneider, 1801, but this taxon was eventually placed in the synonymy of *Leptotyphlops* by Fitzinger (1843). Based on a molecular phylogenetic hypothesis Adalsteinsson et al. (2009) resurrected the genus *Siagonodon*, allocating four taxa that were previously placed in the *Leptotyphlops septemstriatus* species group. This was based on external morphological similarities among these four taxa (*S. borrichianus*, *S. brasiliensis*, *S. cupinensis*, *S. septemstriatus*) proposed by Orejas-Miranda (1967) and Peters (1970), even though only one taxon (*L. septemstriatus*) was included in the molecular analysis. Pinto and Curcio (2011) later transferred *Siagonodon brasiliensis* to *Trilepida* based on external morphology and notably on a new character present in *Trilepida* (presence or absence of fused scales on the dorsal surface of the tail until terminal spine, i.e. = fused caudals). In this same contribution, the authors also described *Siagonodon acutirostris*. Francisco et al. (2018) reviewed the generic contents and proposed six new diagnostic characters for the genus *Siagonodon*, including the presence of a rostral scale with enlarged base, a reduced or absent terminal spine, a straight snout in lateral view, belly unpigmented and short tail. Detailed descriptive osteological studies based on the representatives of the genus *Siagonodon* are missing (List 1966, Cundall and Irish 2008), and so far, there is no available data on the hemipenial morphology for any congener (see Martins et al. 2019a).

Herein we provide the description of a new polymorphic species of the genus *Siagonodon* based on combined morphological and molecular data, and provide the first hemipenial description for the genus. We also reassign *Siagonodon acutirostris* to the genus *Trilepida* based on osteological (skull and lower jaw) data in combination with molecular evidence.

Material and Methods

Taxon sampling and data acquisition

We examined specimens housed in the following institutions (see Appendix 1): Natural History Museum, London, UK (**BMNH**); Coleção Herpetológica da Universidade de Brasília, Brasília, Brazil (**CHUNB**); Instituto Butantan, São Paulo, Brazil (**IBSP**); Field Museum of Natural History, Chicago, USA (**FMNH**); Instituto de Ciencias Naturales, Universidad Nacional de Bogotá, Colombia (**ICN**); Natural History Museum, University of Kansas, Lawrence, USA (**KU**); Los Angeles County Museum, Los Angeles, USA (**LACM**); Laboratório de Zoologia de Vertebrados, Universidade Federal de Ouro Preto, Ouro Preto, Brazil (**LZV-UFOP**); Museum of Comparative Zoology, Cambridge, USA (**MCZ**); Museu Nacional, Universidade Federal do Rio de Janeiro, Rio de Janeiro,

Brazil (MNRJ); Muséum National d'Histoire Naturelle, Paris, France (MNHN); Museu Paraense Emílio Goeldi, Belém, Brazil (MPEG); Museum für Tierkunde in Dresden, Dresden, Germany (MTD); Museu de Zoologia João Moojen de Oliveira, Universidade Federal de Viçosa, Brazil (MZUFV); Museu de Zoologia, Universidade de São Paulo, São Paulo, Brazil (MZUSP); Natural History Museum Vienna, Vienna, Austria (NMW); Museo de Zoología, Pontificia Universidad Católica del Ecuador, Quito, Ecuador (QCAZ); Universidade Federal de Mato Grosso, Cuiabá, Brazil (UFMT); United States National History Museum, Smithsonian Institution, Washington DC, USA (USNM); Zoologische Staatssammlung München, Munich, Germany (ZSM). We provide information on the specimens and localities in Table S1.

We follow Passos et al. (2006), Broadley and Wallach (2007), and Pinto and Curcio (2011) for meristic and pholidosis terminologies. We consider the total number of middorsal scales by excluding the rostral scale and caudal spine, and the number of subcaudals by excluding the caudal spine. Terminology for hemipenial morphology follows Dowling and Savage (1960), as augmented by Myers and Campbell (1981) and Branch (1986). Techniques for hemipenis preparation follow Pesantes (1994), except when examined *in situ*. Measurements were taken with a digital caliper to the nearest 0.1 mm, except for total length (TL) which was taken with a flexible ruler to the nearest 1.0 mm. Sex was determined through a ventral incision at the base of the tail. External morphology characters of other Neotropical leptotyphlopids are based on data from: Passos et al. (2005, 2006), Adalsteinsson et al. (2009), Pinto (2010), Pinto et al. (2010), Pinto and Curcio (2011), Francisco et al. (2012, 2018), Pinto and Fernandes (2012, 2017), and Martins et al. (2019a). The head and cloacal region of three specimens of *Siagonodon* sp. and the paratype of *Siagonodon acutirostris* were X-rayed in 3D with high-resolution μ CT scanning procedures using a Bruker SkyScan 1273 or 1173 at Instituto Alberto Luiz Coimbra de Pós-graduação e Pesquisa de Engenharia (COPPE), Laboratório de Instrumentação Nuclear, Universidade Federal do Rio de Janeiro, Rio de Janeiro. The scans were conducted at an X-ray beam with 40kV source voltage and 180–200 μ A current without the use of a filter, or with an Al 1.0 mm filter. Rotation steps of 0.3–0.5 degrees were used with a frame averaging of 7, recorded over a 180° rotation, resulting in 775–1,574 projections of 312–1,000 ms exposure time each and a total scan duration of 0:42:2–01:11:26s. The μ CT-dataset was reconstructed using N-Recon software (Bruker MicroCT) and rendered in three dimensions through the aid of CTVox for Windows 64 bits version 2.6 (Bruker MicroCT). We used Fiji Software and 3D Slicer and followed Buser et al. (2020) for segmentation. Plates were made using Inkscape 1.0. Comparisons with the skulls of *Siagonodon cupinensis* and *S. septemstriatus* are based on Martins (2016). For obtaining information on the number of precloacal and caudal vertebrae, whole specimens were X-rayed in 2D outside of ethanol with a Faxitron X-ray at Museu Nacional, Universidade Federal do Rio de Janeiro.

Molecular data and phylogenetic analysis

Aiming to assess the phylogenetic position of *Siagonodon* spp. within Leptotyphlopidae, we included representatives of all genera currently included in the Subfamily Epictinae Hedges, Adalsteinsson & Branch, 2009, improving the representativeness of *Trilepida* spp., and representatives of two other basal snake families (Boidae Gray, 1825 and Typhlopidae Merrem, 1820). We selected specific out-group terminals trying to maximize character coverage (i.e., homologous sequences available from GenBank) and phylogenetic structure according to the trees of the two most densely sampled leptotyphlopoid phylogenies (Adalsteinsson et al. 2009; McCranie and Hedges 2016; Martins et al. 2019a). We compiled the complete or partial sequences of eight genes: mitochondrial markers for 12S rRNA (12S), 16S rRNA (16S), cytochrome *b* (*cyt b*); nuclear markers for amelogenin (AMEL), brain-derived neurotrophic factor (BDNF), oocyte maturation factor (C-mos), recombination activating gene 1 (RAG1), and neurotrophin 3 (NT3). Information of the specimens and GenBank accession numbers used in this study is given in Table S2, and identifications followed those from Adalsteinsson et al. (2009), as updated by McCranie and Hedges (2016) and Martins et al. (2019a).

We obtained tissue samples from 17 individuals representing five nominal and one undescribed species: *Siagonodon acutirostris*, *S. cupinensis*, *Siagonodon* sp., *Trilepida dimidiata*, *Trilepida jani*, and *Trilepida salgueiroi*. The new samples were acquired through field work, loans and donations. We checked identifications from all new tissue samples by direct examination of the voucher specimens, comparing such material with type specimens, topotypes and additional comparative material from previously recognized species for accurate identifications. We extracted DNA sequence data by performing PCRs using a PCR Master Mix and a pair of primers for each segment: BDNF forward and BDNF-reverse; NTF3_f1, and NTF3_r1 (Townsend et al. 2008); C-mos S77 and C-mos S78; 12S L1091mod, and 12S H1557mod; 16sar, and 16Sbr (Zaher et al. 2009); *cyt b* 703Botp M13f, *cyt b* MVZ16p M13r (Grazziotin et al. 2012); LAMSQ, Ltyph2L, Ltyph1R (Adalsteinsson et al. 2009), LAM2N (Vidal and Hedges 2005).

Thermocycling for DNA amplification for the first partition began with a denaturation at 94°C (5 min), followed by 40 cycles of denaturation at 94°C (30 s), annealing at 43–48°C (30 s), extension at 70°C (1 min), and a final step at 72°C after the final cycle (7 min). PCR products were visualized in 1% agarose gels and sent to Macrogen Inc. (Seoul, Republic of Korea) for purification and sequencing reactions. PCR products of *Trilepida* spp. were purified with Exosap and sent to Genoma USP — Centro de Estudos do Genoma Humano e Células-Tronco. Resulting electropherograms for both DNA strands were analyzed using Chromas Lite 2.01 and edited using MEGA 6.0 and adjusted manually to generate consensus sequences for each specimen. Sequences were checked with basic

local alignment search tool (Altschul et al. 1997) against the GenBank nucleotide database to ensure that the amplified product was correct and not contaminated.

All sequences were aligned using MAFFT version 7 (Kato et al. 2002), with a gap opening penalty of 1.53 and an offset value of 0.0. Parameters for *cyt b*, AMEL, BDNF, C-mos, RAG1, and NT3 were left at their default settings (L-INS-i model) and parameters for 12S and 16S were set to the E-INS-i model. We aligned each segment separately, and segments were concatenated using Mesquite 3.10, to a total of 5,909 bp. We selected appropriate models of the DNA sequences using the software jModeltest 2.17 (Posada 2008) based on the Akaike information criterion or AIC (Akaike 1974). Obtained models were HKY + G for C-mos, GTR + G for AMEL and RAG1, K80 + G for NT3, GTR + G + I for *cyt b*, BDNF, 12S, and 16S.

We performed partitioned Bayesian Inference (BI) using MrBayes 3.2.2 (Ronquist and Huelsenbeck 2003) through the portal CIPRES Science Gateway (Miller et al. 2010) using the concatenated dataset and the partition models described. Each analysis included four independent runs of 2,000,000 generations with four chains of Markov Chain Monte Carlo. Parameters and trees were sampled every 5,000 generations. We considered convergence of the runs when the standard deviation of the frequency splits was lower than 0.05 and by observing ESS values above 300 in Tracer v1.4 (Rambaut and Drummond 2007). The first 25% of samples were discarded as burn-in. Branch support was assessed by posterior probability, and nodes with posterior probabilities $pp > 0.95$ were considered strongly supported (Matioli and Fernandes 2012).

Species concept and diagnosis criteria

In this study, we followed the general lineage species concept of de Queiroz (2007). We consider presence of one or more exclusive apparently fixed diagnostic characters (either morphological or molecular), which distinguishes a given taxon from the others in the genus *Siagonodon*, as species delimitation criteria. Nonetheless, the sample sizes assessed here were too small for statistical tests and, for that reason, we looked for concordance between the discrete and continuous phenotype characters, as well as corroboration with molecular phylogeny for *Siagonodon* spp. Some of these features are likely uncorrelated, so the correspondence between these kinds of data might represent independent evidence for species boundaries.

Ethics statement

The authors declare that this contribution represents an original work and that no experiment was done with live animals. All specimens pertaining to *Siagonodon* **sp. nov.** were collected under the permits Abio No 1146/2019, Oficio 848/2020/COMIP/CGTEF/DILIC (Brazil) and APA no. 973-23-1 (French Guiana).

Results

Molecular analysis and the generic position of *Siagonodon acutirostris*

The topology recovered based on BI shows that the genus *Siagonodon* (as currently defined) is paraphyletic (Fig. 1), since *Siagonodon acutirostris* is strongly supported ($pp > 0.95$) as the sister-group of the clade *Trilepida jani* + *T. macrolepis* + *T. salgueiroi*. Another instance of paraphyly is recovered within *Trilepida macrolepis*, as the two specimens were nested within different clades. Regarding the genetic distances (16S rDNA) (see Table S2), *S. exiguum* **sp. nov.** had the lowest divergence from its congeners, ranging from 4–7% (S3), except for *S. acutirostris* (with 14–16%). The new species was most genetically close to *S. cupinensis* (4%). Since the nested position of *S. acutirostris* within *Trilepida* implies the paraphyly of both genera, the examination of morphological features of *S. acutirostris* also suggested that it should be assigned to the genus *Trilepida* instead of *Siagonodon*. Thus, we examined the skull of one paratype of *S. acutirostris* (CHUNB 35648; Fig. 2), and noticed that the putative osteological diagnostic data of *Trilepida* proposed by Martins et al. (2021a): i.e., (i) the basioccipital participating in the formation of the foramen magnum, (ii) paired nasals and (iii) fused supraoccipitals are present in *S. acutirostris*. These data contrast with skull data from *Siagonodon* spp. found by Martins (2016) and the present study (see Results: Osteology and Discussion), that report the otooccipitals ventrally in contact and excluding the basioccipital in the formation of the foramen magnum in the genus, added to a conspicuous lateral expansion of the snout, and elongated teeth in the dentary. Therefore, based on the congruence of molecular and morphological data, we transfer *Siagonodon acutirostris* to the genus *Trilepida*, and we will not address this species in the following sections for comparisons with representatives of the genus *Siagonodon*. Further comments can be found at the end of Results and in the Discussion.

Furthermore, the new species of *Siagonodon* is strongly supported ($pp > 0.95$) as the sister species of *S. cupinensis*, and this clade represents the sister-group of *S. septemstriatus* (Fig. 1). The monophyly of four tribes (Epictini, Leptotyphlopini, Myriopholini, and Rhinoleptini) is recovered. All relationships are supported by high posterior probabilities.

New species description

Siagonodon exiguum **sp. nov.**

<http://zoobank.org/CA819359-43BC-4874-B917-9126B29DA619>

Figs 3–11

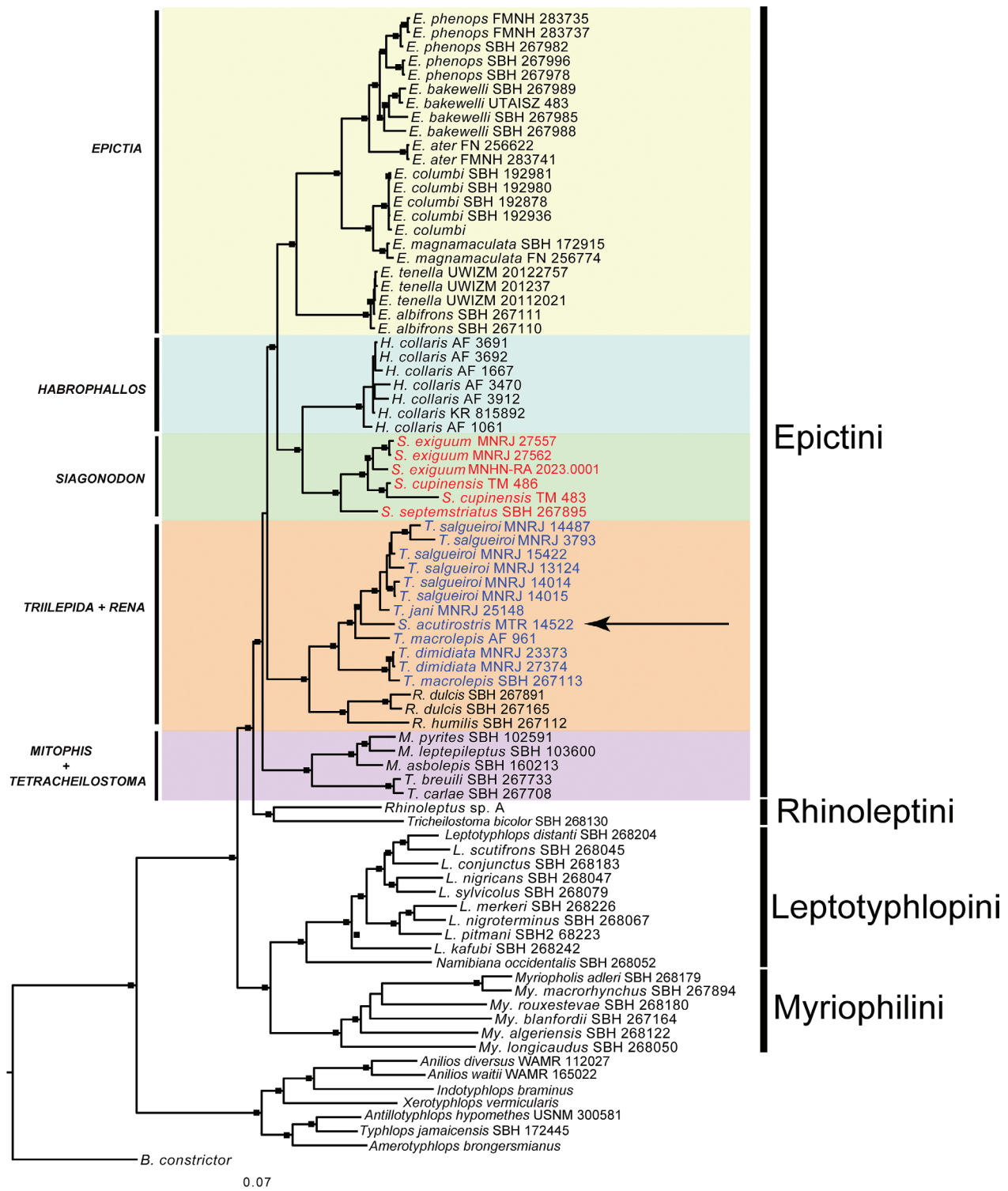


Figure 1. Phylogenetic relationships of Leptotyphlopidae estimated under a Bayesian framework based on eight molecular markers. Only posterior probabilities above 0.95 (>0.95pp) are shown for clarity as black squares at nodes. The arrow indicates the disparate placement of *Siagonodon acutirostris*.

Holotype (Figs 3–5). Adult female, MNRJ 27562 collected on the Monte Branco Plateau located in the Saracá-Taquera National Forest, Pará, Brazil (01°37'56.99"S, 56°33'29.03"W, 195 meters above sea level (m a.s.l)).

Paratypes (Figs 3–5). Six specimens, two females (MNRJ 27557 and 27561) and four males (MNHN-RA-2023.0001, MNRJ 27558–60). MNRJ 27557–61, unknown collec-

tor, from the type locality (01°37'S, 56°33'W); and MNHN-RA-2023.001, collected by T. Decaens and E. Lapied on March 2015, from Mitaraka (02°14'8.77"N, 54°26'57.41"W; 328 m a.s.l), French Guiana.

Diagnosis. The putative autapomorphy of *Siagonodon exiguum* sp. nov. may be represented by lateral pointed projections on the snout or with inconspicuous lateral pro-

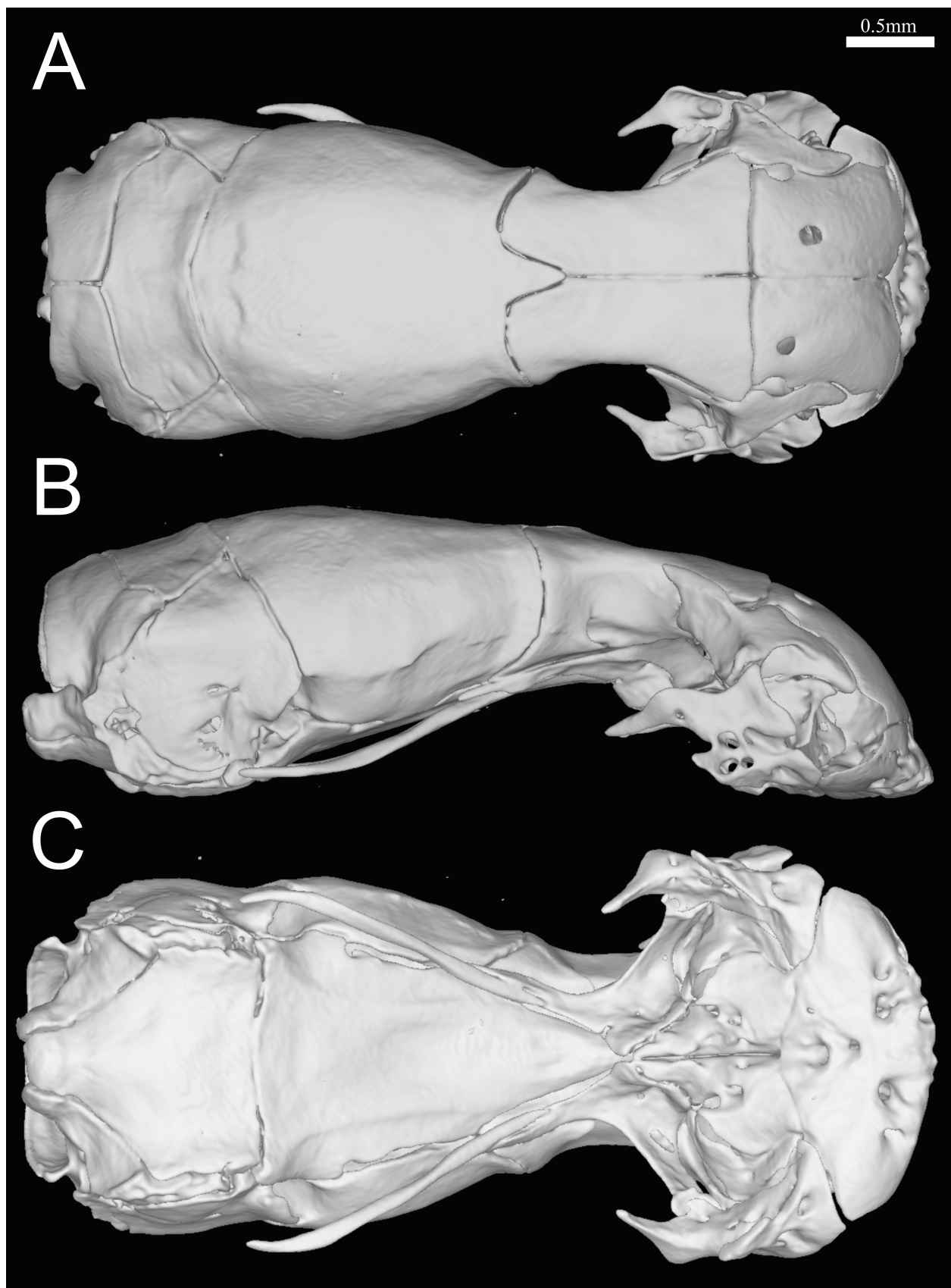


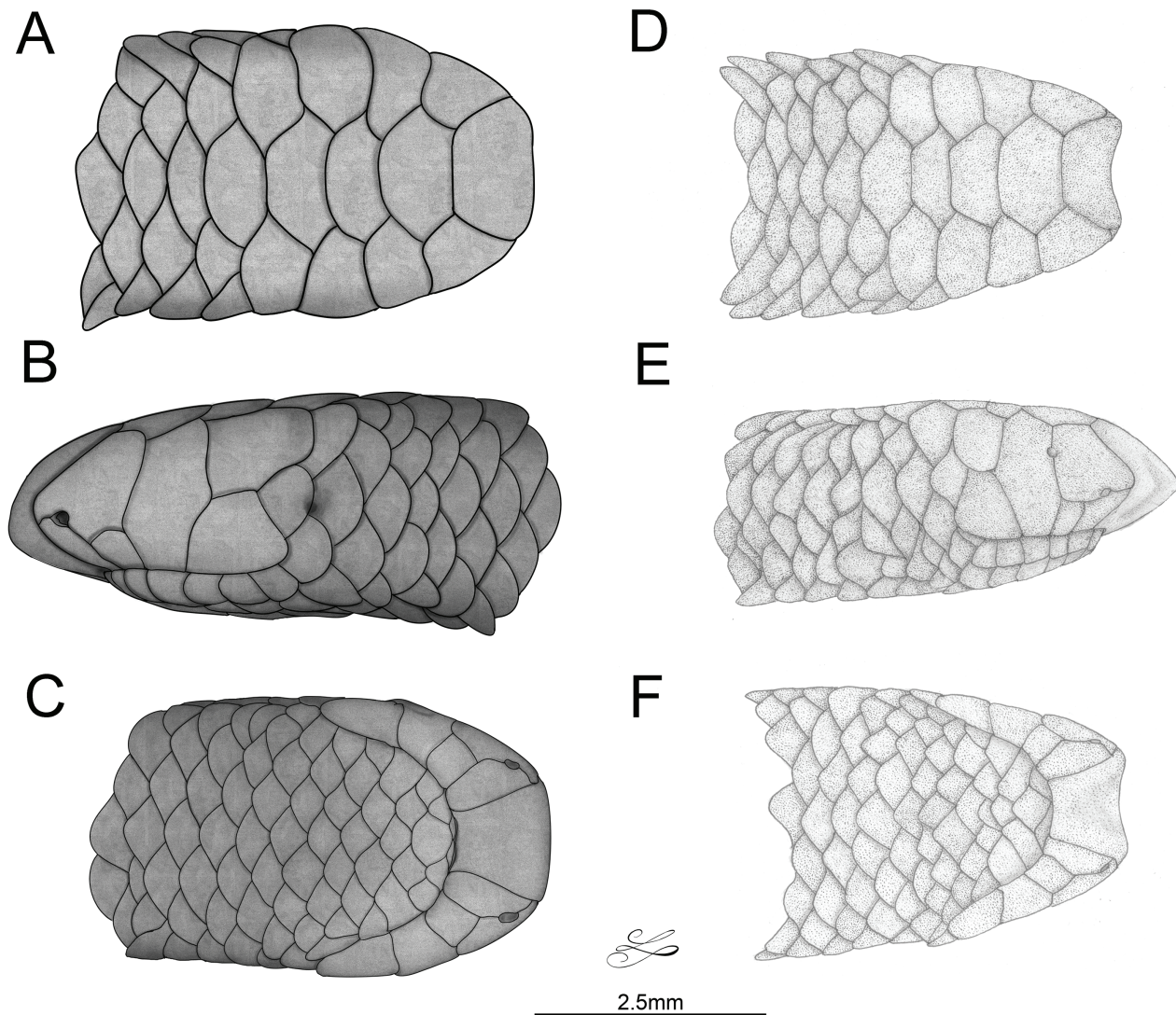
Figure 2. Three-dimensional reconstruction of the skull of *Trilepida acutirostris* based on μ -CT data of the paratype (CHUNB 35648). Dorsal (A), lateral (B), and ventral (C) views.

jection by presenting a slight concavity on the mid-rostral portion of snout (see below in comparison the opposite states for snout condition).

Definition. *Siagonodon exiguum* **sp. nov.** can be distinguished from all congeners by the following combination of external characters: midbody scale rows 14; midtail

Table 1. Comparative meristic data among the species of the genus *Siagonodon*.

Species	Middorsal scales	Midventral scales	Subcaudal scales	Infralabial scales	Midtail scales	Source
<i>S. borrichianus</i>	163–285	245–272	10–13	3	10	Francisco et al. (2018)
<i>S. cupinensis</i>	225–293	224–270	12–16	3–4	14	Francisco et al. (2018); this study
<i>S. exiguum</i> sp. nov.	255–289	230–269	15–18	4	14	This study
<i>S. septemstriatus</i>	213–247	196–237	10–12	4	12	Pinto et al. (2011); Francisco et al. (2018)

**Figure 3.** Dorsal (A, D), lateral (B, E), and ventral (C, F) views of the holotype (MNRJ 27562; Figs A–C) and paratype (MNHN-RA-2023.0001; D–F) of *Siagonodon exiguum* sp. nov.

scale rows 14; supralabials two (1+1); infralabials four; subcaudals 15–18; middorsal scale rows 255–289; total number of preloacal vertebrae 239–263; supraocular scales absent; frontal scale distinct, not fused with rostral; body dorsum and vent uniformly beige; eye totally covered by ocular scale, eye spot un conspicuous and reduced; caudal scales not fused; terminal spine absent; cloacal vertebrae 3–5, caudal vertebrae 18–20, the last one composed of 3 fused vertebrae; snout concave with conspicuous lateral tapered projections, without tapered projections, and slightly concave anteriorly or without projections and truncate anteriorly.

Comparisons with other congeners (conditions for other species in brackets; Table 1). *Siagonodon exiguum* is distinguished from all congeners by the presence (in most specimens) of lateral pointed projections on the snout, or by a slightly concave snout (when present; vs. acuminate in *S. borrichianus*; truncate in *S. cupinensis* and *S. borrichianus* and *S. septemstriatus*); by having 15–18 subcaudal scales (vs. 10–13 in *S. borrichianus*, 12–16 in *S. cupinensis*, and 10–12 in *S. septemstriatus*); by having a pair of optic nerve foramina (vs. single foramen in *S. septemstriatus*); from *S. cupinensis* and *S. septemstriatus* by the fusion of the prootic+otooccipital bones (vs. distinct bones); from

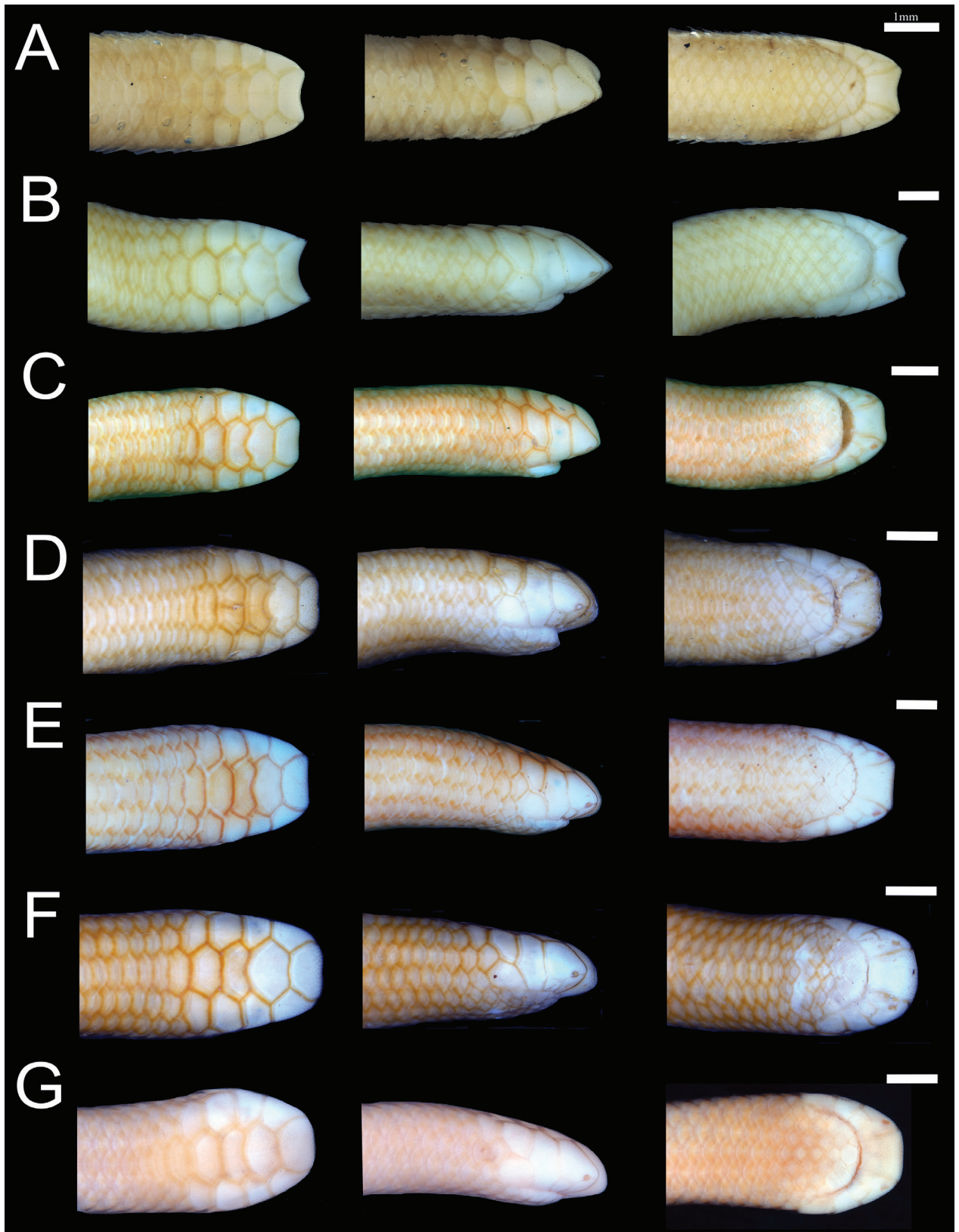


Figure 4. Comparisons of the head in dorsal (left column), lateral (middle column) and ventral (right column) views of the type series of *Siagonodon exiguum* sp. nov. **A** MNHN-RA-2023.0001; **B** MNRJ 27557; **C** MNRJ 27558; **D** MNRJ 27559; **E** MNRJ 27560; **F** MNRJ 27561; **G** MNRJ 27562 (holotype).

S. borrichianus and *S. septemstriatus* by having 255–289 middorsal scales (vs. 163–285 in *S. borrichianus* and 215–244 in *S. septemstriatus*); from *S. borrichianus* and *S. septemstriatus* by having 230–269 midventral scales

(vs. 245–272 in *S. borrichianus* and 196–224 in *S. septemstriatus*); from *S. borrichianus* and *S. septemstriatus* by having 14 scales around midtail (vs. 10 in *S. borrichianus* and 12 in *S. septemstriatus*); from *S. septemstri-*

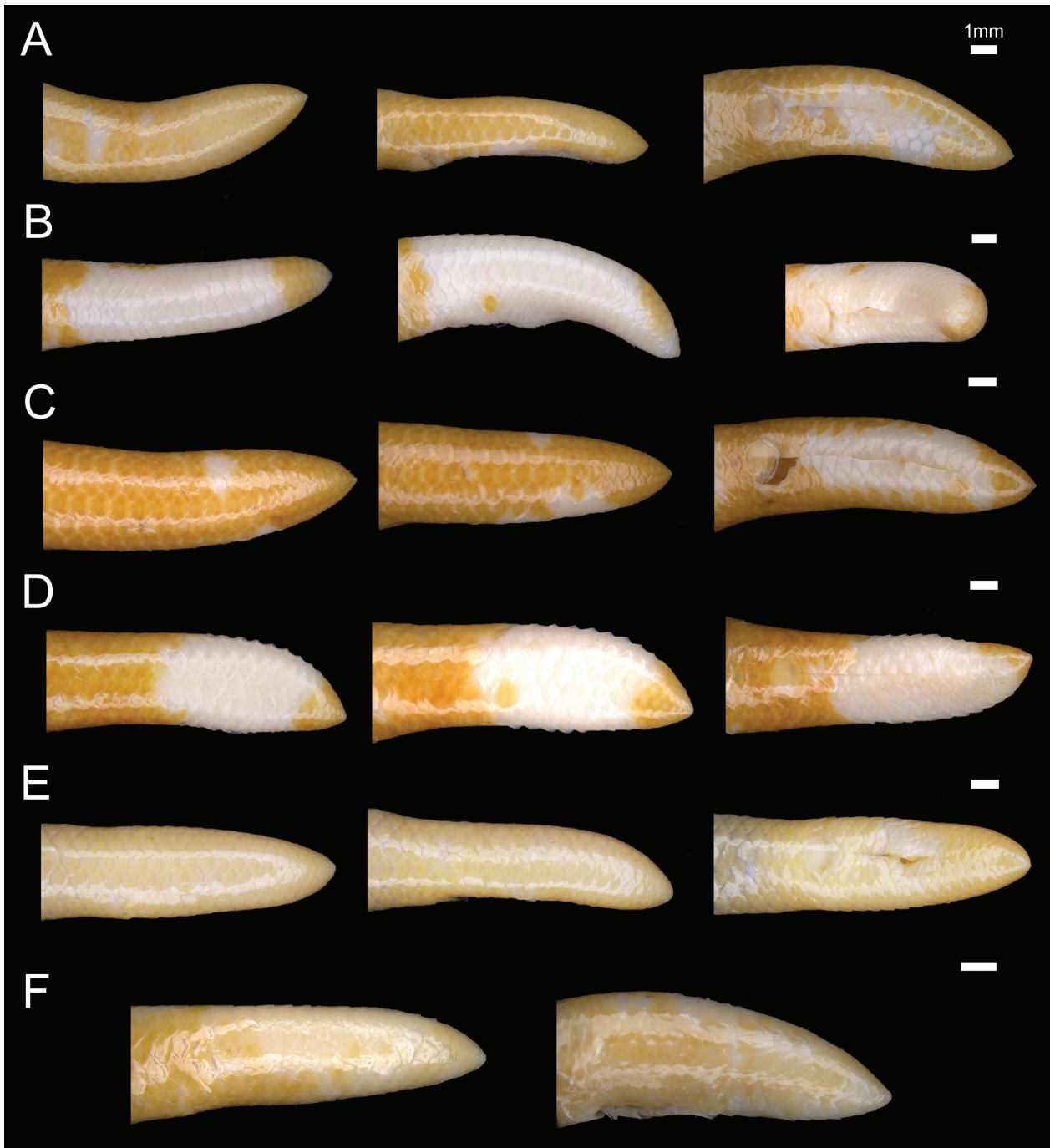


Figure 5. Comparisons of the tail in dorsal (left column), lateral (middle column) and ventral (right column) views of the type series of *Siagonodon exiguum* sp. nov. **A** MNRJ 27558; **B** MNRJ 27559; **C** MNRJ 27560; **D** MNRJ 27561; **E** MNRJ 27562 (holotype); **F** MNHN-RA-2023.0001.

atus and *S. borrichianus* by its uniform beige dorsum and vent color (vs. striped pattern in *S. septemstriatus*, and uniformly dark brown in *S. borrichianus*).

Description of the holotype (Figs 4 and 5). Adult female, Total length (TL) 186 mm, Tail length (TAL) of 8.0 mm; midbody diameter (MB) 3.2 mm; midtail diameter 2.7 mm; TL/TAL 23.2; TL/MB 5.8; rostral width 1.2 mm; inconspicuous eye spot covered by ocular scale; head length 4.9 mm, head width 2.9 mm; head subcylindrical, markedly truncate anteriorly; body subcylindrical, slightly tapered caudally near the tail; head not enlarged,

indistinguishable from neck. Snout truncate in lateral and ventral views; rostral hexagonal in frontal views, and trapezoidal in ventral view; dorsal apex concave, not reaching the anterior limit of oculars; rostral contacting supranasal and infranasal laterally, and frontal dorsally; nasal completely divided horizontally by oblique suture crossing nostril; nostril roughly semicircular, positioned mostly dorsal of nasal suture; supranasal twice as high as long, contacting rostral anteriorly, infranasal ventrally, first supralabial ventrally, ocular posteriorly, and frontal dorsally; supranasal ventral boundary slightly longer than upper border of infranasal scale; infranasal twice as

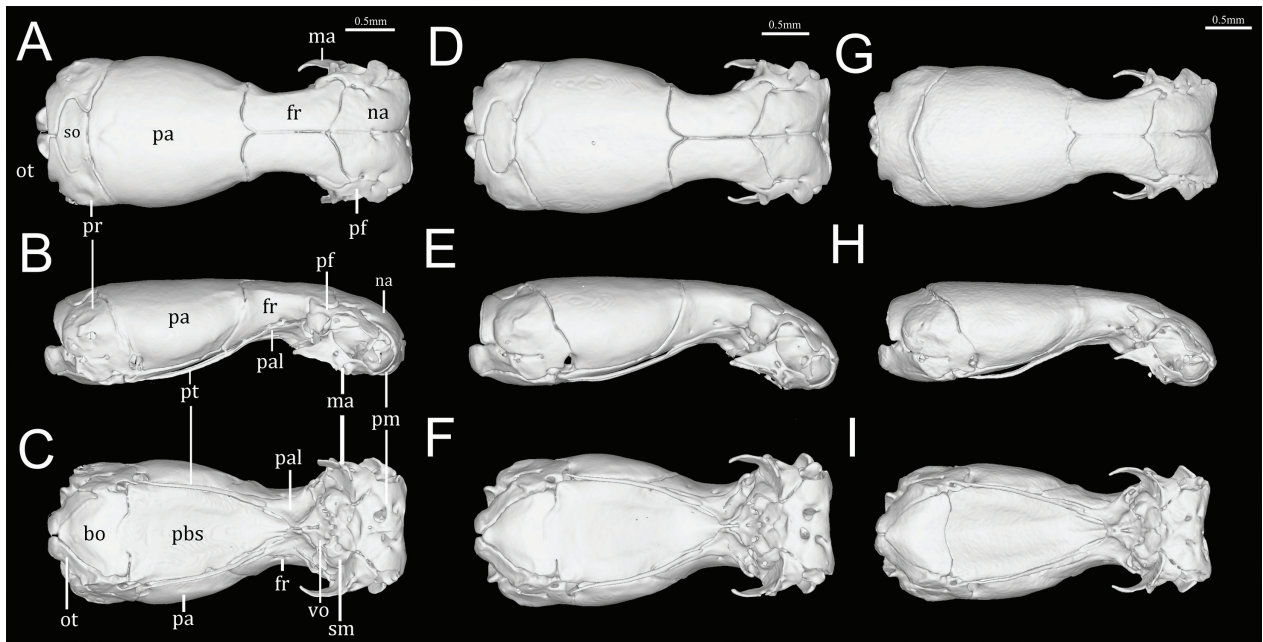


Figure 6. Three-dimensional reconstruction of the skull of *Siagonodon exiguum* sp. nov. based on μ -CT data in dorsal (A, D, G), lateral (B, E, H), and ventral (C, F, I) views. MNRJ 27562 (A–C), MNHN-RA-2023.0001 (D–F), MNRJ 27558 (G–I). Abbreviations: **bo** basioccipital; **fr** frontal; **ma** maxilla; **na** nasal; **ot** otooccipital; **pa** parietal; **pal** palatine; **pbs** parabasisphenoid; **pf** prefrontal; **pm** premaxilla; **pr** prootic; **pt** pterygoid; **sm** septomaxilla; **so** supraoccipital; **vo** vomer.

high as long; upper lip border formed by rostral, infranasal, anterior supralabial, ocular, and posterior supralabial scales; temporal scale not distinct in size from dorsal scales of lateral rows; two supralabials (1+1) entirely separated from each other by ocular; first supralabial about 1.5 times higher than long, not reaching the nostril level or the eye spot; second supralabial roughly semicircular, slightly longer than high, twice as high as first supralabial, its posterior margin in broad contact with temporal; ocular high, dorsal apex acuminate, anterior border straight and vertical, about 3 times higher than long, contacting posterior margins of supranasal and first supralabial anteriorly, parietal posteriorly, frontal and postfrontal dorsally; eye indistinct, covered by ocular scale; eye spot positioned in central area of expanded upper part of ocular, displaced far above nostril level; frontal subcircular, slightly wider than the other middorsal head plates (postfrontal, interparietal, and interoccipital); middorsal head plates (postfrontal, interparietal, and interoccipital) subequal in size, trapezoidal in dorsal view, weakly imbricate; frontal enlarged, about twice as wide as long, contacting rostral, supranasals, oculars, and postfrontal; postfrontal about twice as wide as long, contacting frontal, oculars, parietals, and interparietal; interparietal twice as wide as long, contacting postfrontal, parietals, occipitals, and interoccipital; interoccipital about as wide as long, contacting interparietal, occipitals, and first dorsal scale of vertebral row; parietal hexagonal, about as wide as long; lower margin contacting upper border of second supralabial, posterior margin contacting temporal, occipital, and interparietal, anterior margin in broad contact with ocular and postfrontal; occipital almost twice wider than long, its lower limit attaining level of upper margin of second supralabial, although separated from

the latter by temporal; symphyseal subcircular, anterior and posterior borders respectively straight and slightly convex, about twice wider than long; four infralabials; first infralabial small, subtriangular; second and third infralabials subequal, wide, somewhat higher than long, not pigmented; fourth infralabial twice longer than high high, distinctively longer than others, as high as second and third supralabial, not pigmented; dorsal scales homogeneous, cycloid, smooth, slightly imbricate, arranged in 14 scale rows around midbody and in the middle of the tail; middorsal scales 289; midventral scales 266; cloacal shield short and semicircular, almost twice as wide as long; 16 subcaudals; fused caudals absent; terminal spine indistinct or absent.

Coloration of holotype relatively faded after preservation; dorsal, paraventral and ventral scales uniformly beige; dorsal and ventral head shields creamish white; cloacal shield creamish white.

Osteology. Skull (Fig. 6; $n = 3$; holotype condition indicated with asterisk). Premaxilla wide, expanded anterolaterally, roughly rectangular ($n = 2^*$) or trapezoidal ($n = 1$) in anterior view; and triangular in ventral view, edentulous, pierced by seven ($n = 2$) or eight ($n = 1^*$) foramina; nasal process of premaxilla reduced and tapered toward apex, transverse process absent and vomerian process tapered and single; premaxilla with internal septum composed of two laminae that support the septum nasi dorsally, expanding posteriorly and contacting septomaxilla ventrally; nasals paired, elongated, expanded anterolaterally, with convex anterior limit, and undulated dorsoposterior suture with frontals; being pierced by pair of foramina in posterolateral border of contact with prefrontals and frontals (foramen for the apicalis nasi); additional pair of

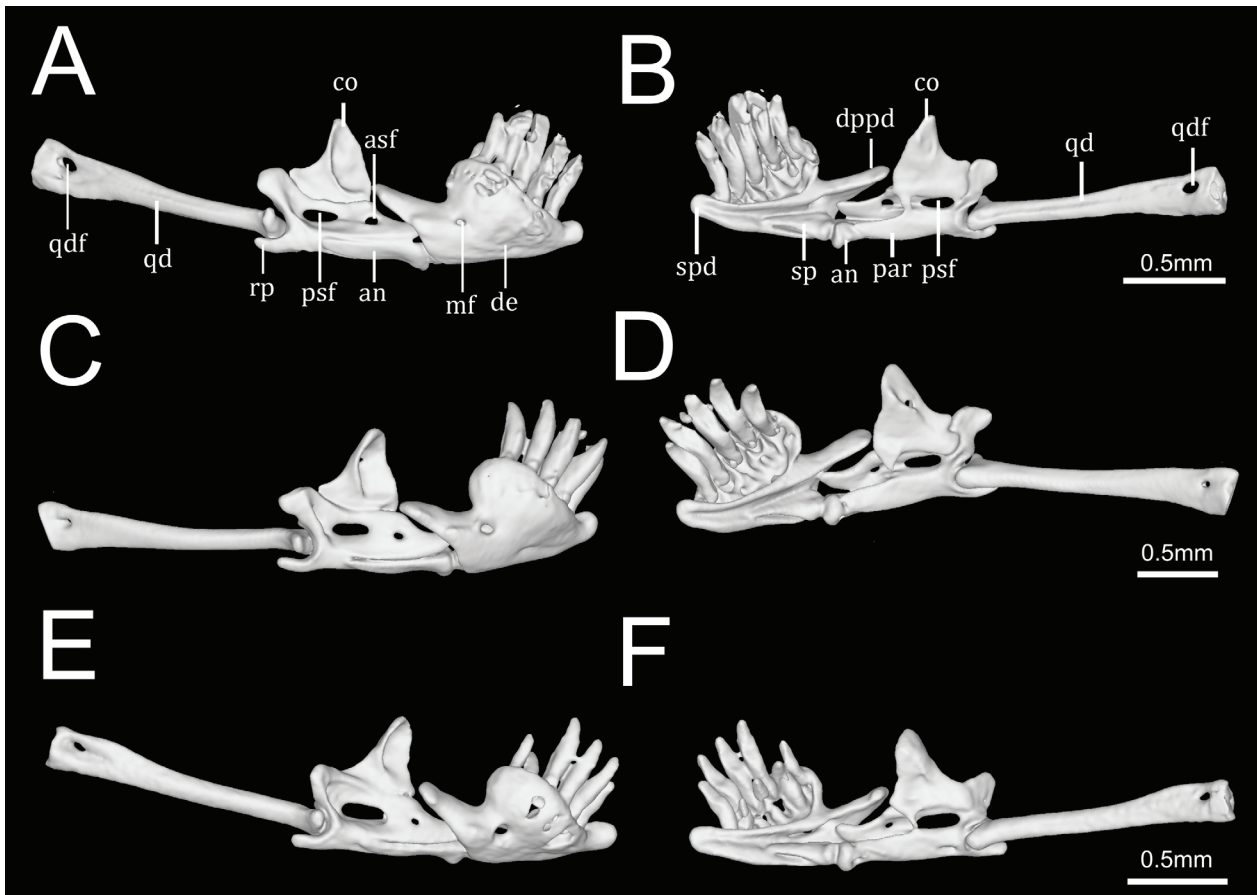


Figure 7. Three-dimensional reconstruction of the lower jaw of *Siagonodon exiguum* sp. nov. based on μ -CT data in lateral (A, C, E) and medial (B, D, F) views. MNRJ 27562 (A–B), MNHN-RA-2023.0001 (C–D), MNRJ 27558 (E–F). Abbreviations: **an** angular; **asf** anterior surangular foramen; **co** coronoid; **de** dentary; **dppd** dorsoposterior process of dentary; **mf** mental foramen; **par** prearticular lamina of compound bone; **qd** quadrate; **qdf** quadrate foramen; **rp** retroarticular process; **sp** splenial; **spd** symphyseal process of dentary.

foramina pierce on the medial contact within both nasals; nasal septum descending as double medial vertical flanges that contact premaxilla and septomaxilla ventrally (internally); prefrontals paired, irregular in shape, in contact with septomaxilla midventrally, and separated by short gap ($n = 2^*$) from maxilla ventrolaterally or in contact with it ($n = 1$); each prefrontal perforated by two ($n = 2^*$) or three ($n = 1^*$) foramina; septomaxillae paired, complex in shape, expanding dorsoanteriorly and comprising posterior limit of naris; conchal invagination absent; ascending process of premaxilla pierced by single large foramen ($n = 2^*$) or by two foramina ($n = 1$); internally, dorsal surface of each septomaxilla pierced by single foramen ($n = 3$ sides*) or two foramina ($n = 3$ sides*), and with medial inconspicuous sulcus ($n = 2^*$), or sulcus absent ($n = 1$); vomers paired, located midventral to vomeronasal cupola, transversal arms absent, with posterior arms in contact with each other posteriorly ($n = 2^*$) or not ($n = 1$); pair of foramina pierce the ventral lamina of each vomer; frontals paired, elongated, approximately twice longer than wide, both elements bearing short anterolateral projections to attach to prefrontals; frontal pillars absent; optic nerve foramen paired ($n = 2^*$) or single ($n = 1$), restricted to lateral descending surface of frontals; maxilla edentulous, irregular in shape, pierced by four ($n = 1^*$) or

six ($n = 2$) foramina; posterior process of maxilla reaching ($n = 1$) or not reaching ($n = 2^*$) level of anteriormost optic nerve foramen in lateral view; posterior orbital element absent; parietal single, wide, representing largest bone of braincase; parietal internal pillars (sensu Martins et al. 2021a) present; parabasisphenoid arrow-like, with tapered anterior tip lying dorsally to palatine, and fitting in medial line of vomeronasal cupola; posterior limit of parabasisphenoid convex medially; internal (dorsal) face of parabasisphenoid with inconspicuous lateral sulci; anterior opening for palatine artery indistinct or absent; internal carotid artery foramen and abducens nerve foramen present; opening for palatine ramus of facial nerve formed by lateral edge of parabasisphenoid and ventral edge of parietal; basioccipital single and approximately triangular in ventral view, lateral process for attachment of tendons for nuchal muscles (Martins et al. 2019b) absent; basioccipital does not participate in formation of foramen magnum; supraoccipitals fused into single unit, approximately twice wider than long; prootics fused to otooccipitals; prootics+otooccipitals forming trigeminal nerve foramen together with parietal and parabasisphenoid (on one side of one specimen parabasisphenoid does not participate in it); prootics pierced medially (internally) by single acoustic nerve foramen; two statolyth

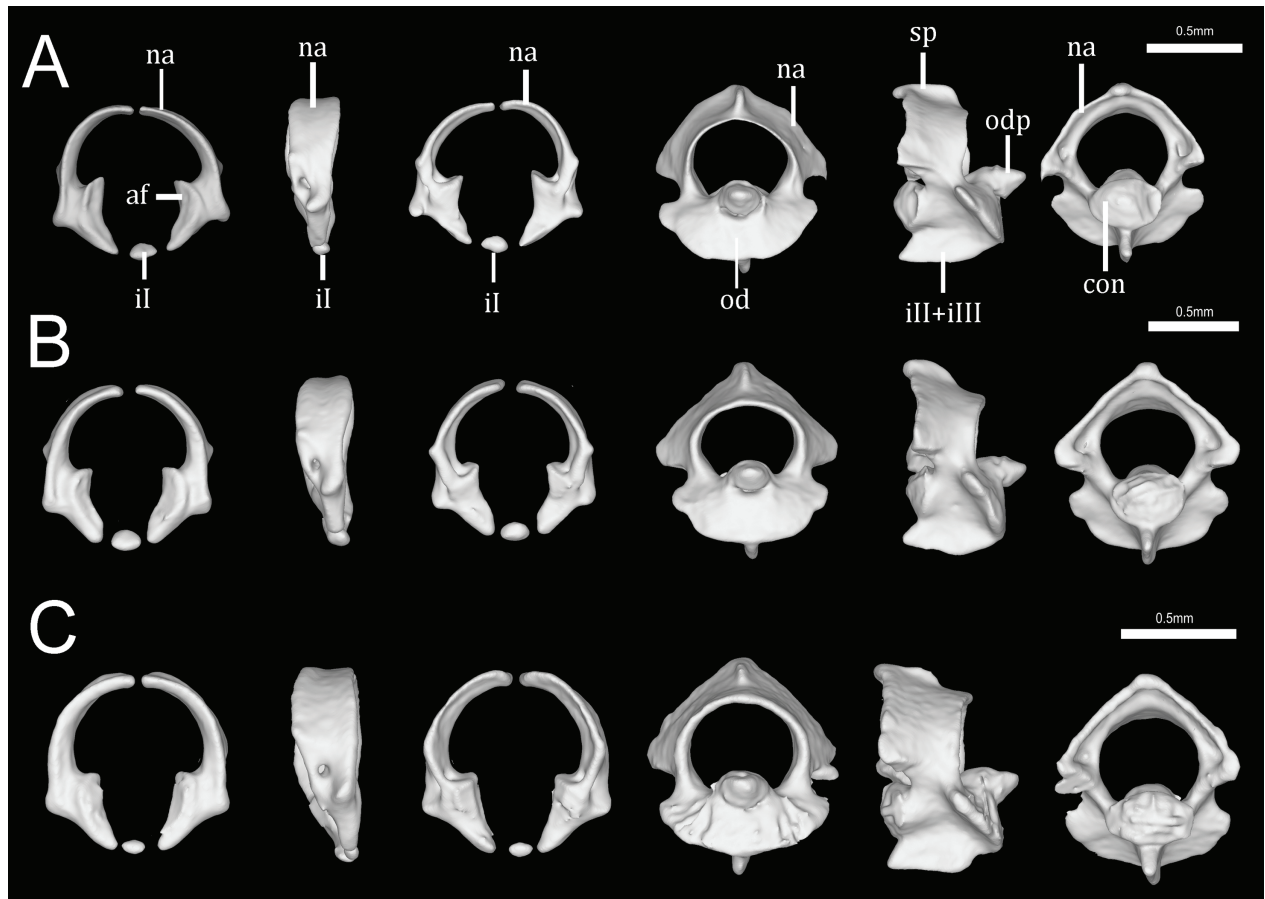


Figure 8. Three-dimensional reconstruction of the atlas (first to third column) and axis (fourth to sixth column) of *Siagonodon exiguum* **sp. nov.** in anterior, lateral and posterior views based on μ -CT data. MNRJ 27562 (A), MNHN-RA-2023.0001 (B), MNRJ 27558 (C). Abbreviations: **af** articular facet; **con** condile; **il** intercentrum I; **iII** intercentrum II; **iIII** intercentrum III; **na** neural arch; **od** odontoid; **odp** odontoid process; **sp** spinal process.

masses present in cavum vestibuli ($n = 2^*$) or statolythic mass absent; stapedia footplate apparently not co-ossified with prootic; otooccipitals dorsally forming short but distinct atlantal process; descend to ventral midline and contact each branch ventrally to exclude basioccipital in formation of foramen magnum; medial surface (internal) of otooccipitals+prootics pierced by internal opening for recessus scalae tympani, perilymphatic foramen, posterior vagus nerve foramen, and reduced foramen that might represent hypoglossal nerve passage; palatines paired and triradiate; anterior margin of maxillary process flexing ventrally and contacting prefrontal ($n = 2^*$) or not ($n = 1$); each palatine pierced by a foramen in its ventral surface; pterygoids slender and rod-like, not contacting quadrate posteriorly, and not extending beyond anterior margin of basioccipital; ectopterygoid indistinct.

Suspensorium (Fig. 7; $n = 3$; holotype condition indicated with asterisk). Dentary supports series of five long teeth ankylosed to inner surface of medial margin of dental concha; mental foramen nearly under fifth tooth; dorso-posterior process of dentary with rounded enlargement ($n = 1$), possibly to provide attachment for *Musculus ceratmandibularis* and/or to *Musculus cervicomandibularis* (Martins et al. 2019b) or not as above ($n = 2^*$); splenial conical, visible in lateral view, representing smallest bone

in lower jaw, extending from level of third tooth to contact angular posteriorly; anterior mylohyoid foramen absent on splenial; posterior mylohyoid foramen on ventral surface of angular; angular conical, extending posteriorly to level of posterior surangular foramen; compound bone pierced by two foramina on surangular lamina, posterior elliptical and wide, anterior small and rounded; anterior surangular foramen located slightly anterior to coronoid; foramen for chorda tympani of hyomandibular ramus of facial nerve (VII) present ($n = 2^*$) or indistinct ($n = 1$); foramen of retroarticular process absent; prearticular lamina of compound bone presenting dorsal process to support coronoid ($n = 1$) or not ($n = 2^*$); coronoid wide, approximately triangular in shape, about as wide as tall, pierced by foramen in its medial side ($n = 2^*$) or not ($n = 1$); quadrate long and slender, about 50% of skull length, posterior process absent (sensu Martins 2016); dorsal foramen in anterior half of quadrate absent; dorsoanterior lamina of quadrate with shallow sulcus that extends throughout half its extension ($n = 2^*$) or not ($n = 1$).

Cervical vertebrae ($n = 3$; holotype condition indicated with asterisk; Fig. 8). Atlas composed of neural arches, not fused dorsally or ventrally; ventral element (intercentrum I sensu Holman 2000) reduced and not fused to neural arches; lateroposterior process of atlas

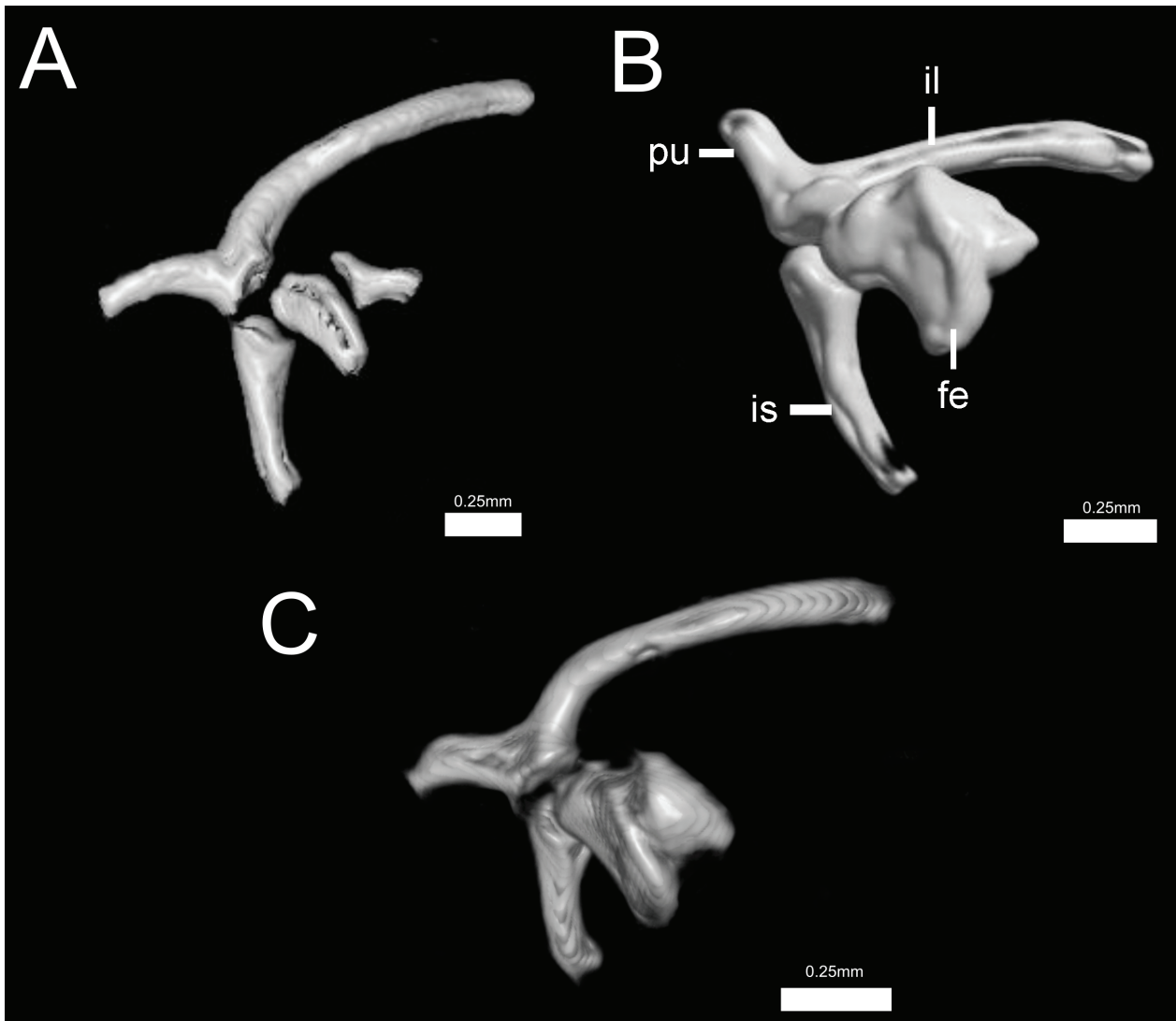


Figure 9. Three-dimensional reconstruction of the pelvic rudiments of *Siagonodon exiguum* sp. nov. based on μ -CT data. MNRJ 27562 (A), MNHN-RA-2023.0001 (B), MNRJ 27558 (C). Abbreviations: fe femur; il ilium; is ischium; pu pubis.

present; axis with inconspicuous spinal process that projects both dorsally and posteriorly; lateral foramina of axis (centrum) indistinct or absent; short lateral processes present ($n = 2$) or absent ($n = 1^*$). Odontoid process of axis osseous and sutured to axis, approximately lozenge shaped in anterior view, with an anterior tapered process; intercentra II and III (sensu Holman 2000) fused into a single unit, compressed laterally.

Pelvic girdle ($n = 3$; holotype condition indicated with asterisk; Fig. 9). Composed of ilium, ischium, femur, and pubis. Ilium and pubis rod-like; ischium approximately rectangular and fused to pubis ($n = 1$) or ischium rod-like and not fused to pubis ($n = 2^*$); ilium represents longest bone of pelvic girdle, being fused to pubis ($n = 2^*$) or not ($n = 1$); femur approximately rectangular and curved with dorsolateral claw-like process ($n = 2^*$) or without such process ($n = 1$).

Hyoid ($n = 3$). Hyoid Y-shaped, extending from 8–11th (MNHN-RA-2023.0001), 10–14th (Holotype), or 11–14th vertebrae. Lingual process distinctively shorter than cor-

nua, with the former being approximately one vertebra long.

Hemipenis (paratype MNRJ 27560, $n = 1$) (Fig. 10). Fully everted and almost maximally expanded hemipenis (examined ex-situ) renders a unilobed organ, about 2 mm long, slightly broadened at base, followed by a short tapered area that posteriorly expands towards apex; basal portion not ornamented on proximal half; hemipenial body with no ornamentation on either sulcate or asulcate sides; sulcus spermaticus single, entering organ on basal surface and extending toward apex of organ; sulcal folds raised and not ornamented; distal half of hemipenial body covered by three inconspicuous transverse flounces; organ apex convex and not ornamented; single and tapered projection develops from apex of asulcate side.

Meristic and morphometric variation. Middorsal scales 285–289 (287 ± 2.8 ; $n = 2$) in females and 255–280 (269 ± 12.5 ; $n = 4$) in males; midventral scales 266–267 (266.5 ± 0.7 ; $n = 2$) in females and 230–269 (253 ± 16.4 ; $n = 4$) in males; subcaudals 15–16 (15.5 ± 0.7 ; $n = 2$) in

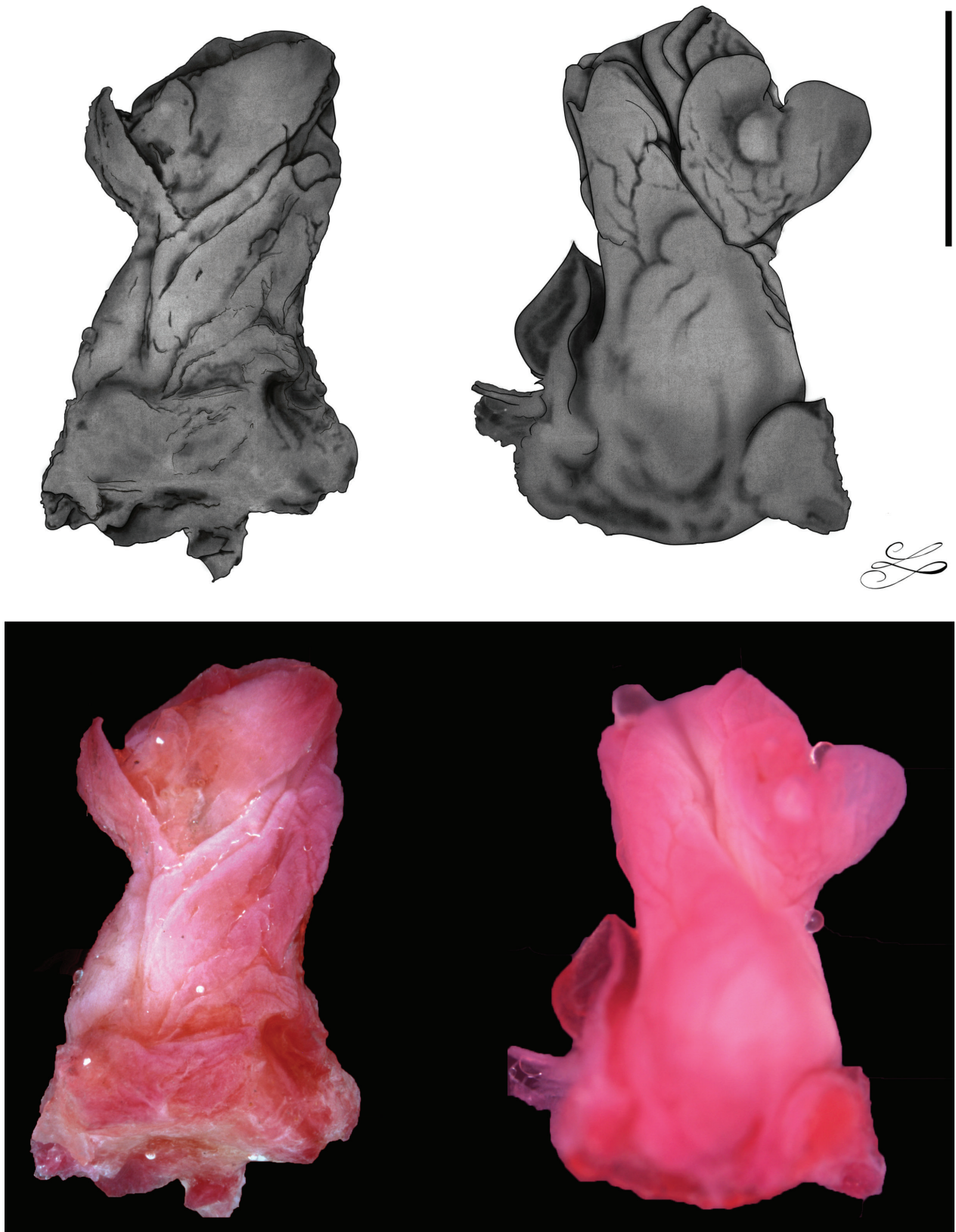


Figure 10. Schematic illustrations (upper line) and photos (lower line) of the asulcate (left) and sulcate (right) sides of the hemipenis of *Siagonodon exiguum* sp. nov. (MNRJ 27560).

females and 16–18 (17 ± 0.8 ; $n = 4$) in males; TL 184–204.2 (195.1 ± 12.9 ; $n = 2$) in females and 171.1–200.3 (187.1 ± 12 ; $n = 4$) in males; TL/TAL ratio 20.0–23.2 (21.6 ± 2.2 ; $n = 2$) in females and 19.4–22.5 (20.6 ± 1.5 ; $n = 4$) in males; TAL 4.3–4.9% of TL (4.6 ± 0.5 ; $n = 2$)

in females and 4.4–5.1% (4.9 ± 0.3 ; $n = 4$) in males; TL/midbody diameter 2.4–3.1 (2.7 ± 0.5 ; $n = 2$) in females and 2.3–2.8 (2.6 ± 0.6 ; $n = 4$) in males; TAL/midtail diameter 2.8–3.5 (3.1 ± 0.4 ; $n = 2$) in females and 2.5–3.4 (3 ± 0.3 ; $n = 4$) in males.

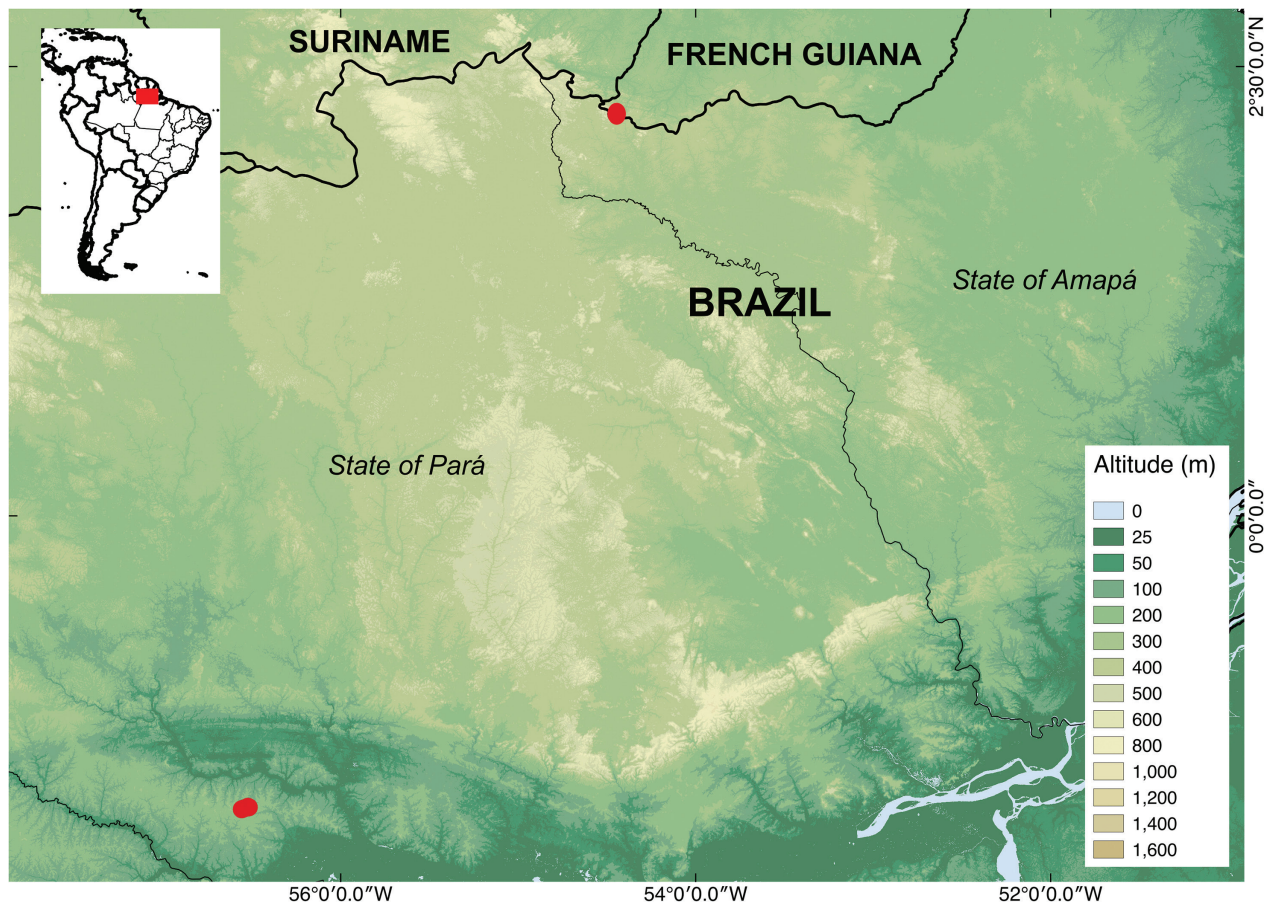


Figure 11. Distribution map of *Siagonodon exiguum* sp. nov. based on the type series (7 specimens).

Color pattern variation. Color pattern of paratypes mostly resembles that of holotype except for the following: dorsum and vent uniformly light brown in three paratypes (MNRJ 27559–61).

Postcranial quantitative variation. Preloacal vertebrae 248–260 (254 ± 8.5 ; $n = 2$) in females and 239–263 (253 ± 10 ; $n = 4$) in males; cloacal vertebrae 4–5 (4.5 ± 0.7 ; $n = 2$) in females and 3–4 (3.5 ± 0.6 ; $n = 4$) in males; caudal vertebrae 18 in females ($n = 2$) and 18–20 (19.2 ± 0.9 ; $n = 4$) in males.

Etymology. The specific epithet *exiguum* is a Latin word meaning little, short, scanty and/or poor. Although readers might think that the name was chosen in allusion to the small size of the species, we dedicate the species to all minorities in science including gender, race/color, ethnicity, and sexual orientation that are considerably underrepresented in the academia throughout the world, especially in higher positions. Although several worldwide initiatives have been implemented in the past few years, the scientific environment is still biased, discouraging and, sometimes noxious, largely because of persisting systemic social, economic and cultural aspects.

Distribution and Natural History (Fig. 11). *Siagonodon exiguum* is currently known from the type locality in Pará State (Brazil) and French Guiana (Mitaraka, Nouragues – A. Fouquet pers. obs and Angouleme –

Dewynter et al. 2020). In Brazil, the species was found during plant suppression in “Terra Firme” (non-flooded forest) forests on the Monte Branco Plateau. The plateau is part of the Saracá-Taquera National Forest, a Sustainable Use Conservation Unit where bauxite mining activities take place, in the municipality of Oriximiná, at 190–200 m altitude. The known occurrences lie within the Guiana Region (Vacher et al. 2020) which correspond to the lowland of the Eastern part of the Guiana Shield. The specimen from Mitaraka was found when digging in search for earthworms.

The X-ray images of two specimens (MNRJ 27558 and 27562) revealed the presence of dense and granular digestive content over half of the specimens’ snout-vent length. In MNRJ 27562, however, X-ray images most likely reveal the presence of at least six elongated eggs, with both anterior and posterior margins hardly delimited. Images also seem to reveal the presence of what seems to represent an embryo in the anteriormost egg (see Supplementary Material 3, X-ray images).

New combination. Pinto and Curcio (2011) described *Siagonodon acutirostris* based on a combination of morphological characters, including a new character for the diagnosis of the genus. Martins (2021a) proposed the following osteologically diagnostic characters for the genus *Trilepida* based on a high sample of species: (i) the basioccipital participating in the formation of the foramen magnum, (ii) paired nasals and (iii) fused supraoccipitals.

Based on the combination of morphological characters proposed by Adalsteinsson et al. (2009), Pinto and Curcio (2011), and Martins (2016, 2021a), and the molecular data provided herein, we propose a new combination and new diagnosis for *S. acutirostris* and regard the presence of fused caudals as a homoplastic character.

***Trilepida acutirostris* (Pinto & Curcio, 2011) new combination**

Siagonodon acutirostris Pinto & Curcio, 2011:58 (CHUNB 35648, holotype, from the municipality of Almas, state of Tocantins, Brazil).

Siagonodon acutirostris – Wallach et al. 2014: 665.

Siagonodon acutirostris – Nogueira et al. 2019.

Definition and Diagnosis. *Trilepida acutirostris* is distinguished from all Neotropical leptotyphlopids by the following unique combination of characters: snout slightly acuminate in lateral and ventral views; absence of supraocular scale; middorsal cephalic plates distinctively enlarged; ocular scale subheptagonal, dorsal apex acuminate and anterior border straight, roughly vertical at eye level; first and second supralabial scales not reaching eye level; two supralabials (1+1); fused caudals absent; temporal scale not distinct; rostral subcircular in dorsal view; middorsal scales 169–183; midventral scales 161–173; subcaudal scales 9–11; 12 scales around the middle of the tail; dorsum uniformly pale copper on five dorsal scale rows, contrasting with the whitish cream tonality covering nine scale rows of venter, and thereby reaching the paraventral region of trunk. Osteology characters: the basioccipital participating in the formation of the foramen magnum, paired nasals and fused supraoccipitals.

Discussion

The fossorial snakes of the Family Leptotyphlopidae (approximately 140 nominal extant species; Uetz et al. 2022) usually exhibit an extremely conserved external morphology (Martins et al. 2021a) and are among the least known terrestrial vertebrates (Marin et al. 2013). Although molecular evidence has helped in determining their higher-level relationships (Adalsteinsson et al. 2009), such data have rarely been useful for unambiguous diagnosis among genera (Martins et al. 2019a), which were defined based on general resemblance (i.e., external morphology) of traditional species groups (see Orejas-Miranda 1967; Peters and Orejas-Miranda 1970). On the other hand, several leptotyphlopoid studies have brought magnificent evidence derived from the internal morphological systems (i.e., bones, cartilages, muscles, glands, visceral anatomy and genitalia), contributing decisively to re-positioning many taxa in the tree of life (Martins et al. 2019a, 2019b, 2021a, 2021b; Koch et al. 2021). In addition, a few taxonomic decisions based on the external morphology characters (e.g., Pinto and Fernandes 2012) have been also

corroborated by new molecular phylogenies (distinctiveness of *T. jani* and *T. dimidiata*; Fig. 1).

By contrast, other generic allocations (e.g., *Siagonodon borrichianus* and *Rena* spp.) still require to be confirmed through congruence between new anatomical approaches (Martins et al. 2018, 2019a; Koch et al. 2021) and molecular evidence (e.g., transference of *Siagonodon acutirostris* to the genus *Trilepida*; present study; Figs 1, 2). The allocation of *Siagonodon acutirostris* in the genus *Trilepida* (present study) was based on osteological + molecular data. The species was described by Pinto and Curcio (2011) and the allocation of *T. acutirostris* in the genus *Siagonodon* was based considering that the taxon fitted the expanded diagnosis provided for both *Trilepida* and *Siagonodon*. Some of those characters are in fact not exclusive to *Siagonodon*, and some reveal a polymorphic condition in some species (*T. brasiliensis*), like the presence/absence of a supraocular scale (see Pinto and Curcio 2011). Even though the presence/absence of a supraocular scale represents a polymorphic character among *Siagonodon* (see Francisco et al. 2018), its presence/absence in representatives of the genus *Trilepida* has only been reported for *T. brasiliensis*, a condition which is shared with *T. acutirostris*. Pinto and Curcio (2011) also described a new character attributed to Neotropical groups, notably fused caudal scales, that according to the authors are present in *Trilepida* species but absent in *Siagonodon* species. The unfused caudal scales in *Trilepida acutirostris* suggest that this character is also homoplastic.

Besides the phenotypic and molecular evidence herein provided for the allocation of *S. acutirostris* in *Trilepida*, additional meristic characters also seem to support the distinctiveness between *Siagonodon* and *Trilepida*. For instance, *Siagonodon* spp. (except for *S. borrichianus*) present a higher middorsal scale count (196–293; see Table 1) in comparison to *Trilepida* spp., (152–253; Adalsteinsson et al. 2009; Pinto et al. 2010; Pinto and Curcio 2011; Salazar-Valenzuela et al. 2015; Pinto and Fernandes 2017). This pattern is also found in *T. acutirostris*, which exhibits a lower middorsal scale count (169–183). Finally, although projecting snouts are common in several leptotyphlopoid species (e.g., *S. borrichianus*, *Rena unguirostris*), *Trilepida acutirostris* currently represents the only known species of the genus with such a modified snout.

The burrowing lifestyle has been repeatedly associated with phenotype conservativeness in fossorial lineages in general, including ‘Scoleophidia’ (Miralles et al. 2018), which may be imposed by some level of morphological stasis due to stabilizing selection, reducing morphological change that usually accompany speciation (see Bickford et al. 2006). However, there are several other reasons why phenotype disparity accompanies speciation such as: recently diverged species, adaptative convergence, or stasis (Struck et al. 2018). Not surprisingly, a general pattern that emerges from most molecular studies suggests a high level of cryptic diversity (= candidate species) in three main ‘scoleophidian’ phylogenetic branches (Anomalepididae, Leptotyphlopidae and Typhlopoidea) (Marin et al. 2013; Miralles et al. 2018; Santos and Reis

2018, 2019). Notwithstanding, to identify and quantify species that are cryptic from those that are not, detailed information about phenotypic disparity must be related to genetic divergence, levels of gene flow, reproductive isolation and phylogenetic niche conservatism (Struck et al. 2018). In the case of *Siagonodon exiguum* **sp. nov.** we found a 4% mt DNA (16S) divergence between the individual from French Guiana in comparison with specimens from Brazil. However, the examination and combination of genetic data with all other morphological data (both external and internal) provided herein does not indicate (considering the current available data) this individual as phenotypically distinct, and the character states combination that is diagnostic for the species is present in both samples (including snout projections and osteological characters that distinguishes the specimen from other *Siagonodon* spp.).

Conversely, specimens from the same locality in Brazil show a low mtDNA variation (<2%), but exhibit different snout shapes (pointed vs. not pointed). Even though recent studies (e.g., Markolf et al. 2011) have suggested lineage separation for species with low genetic distance and high morphological variation, there is no additional evidence (= congruence of data) herein that might suggest that the snout variation is indicative of lineage divergence, or that other associate phenomena explain this snout variation, such as allometric ontogeny and secondary sexual dimorphism. Future additional samples (individuals and DNA) might help understand the data found herein (i.e., morphological variability and genetic structure), since samples per locality are still low, and consideration of genetic distance alone without any additional evidence should be examined with caution. Nevertheless, the morphological variation (= polymorphism) found herein is considered as a paradox in threadsnakes, since this group has historically considered morphologically similar, and that snout variation is found even with low genetic distances from specimens from the same locality.

We provide the first hemipenial description for any of the currently known species of the genus *Siagonodon*. The organ morphology does not resemble any of the known hemipenes amongst Epictinae (see Wallach, 2016, Martins et al. 2019a and Ferreira et al. 2021) in being totally naked and bearing a tapered projection at the asulcate side. Such a projection is also present in its sister taxon (*Habrophallos collaris*; Martins et al. 2019a; see Fig. 10) although in the latter it is doubled and projected towards the base of the organ. Further hemipenial descriptions of *Siagonodon* species are still needed to provide detailed data that assist any systematic assumption (i.e., putative diagnostic characters) for the genus.

Finally, *Siagonodon exiguum* is probably endemic to the Eastern Guiana Shield (Guiana region of Vacher et al. 2020), a region with well-preserved areas, mainly due to low population densities and limited infrastructures (Hollowell and Reynolds 2005). The endemism of this amazonian subregion is very high (anurans: Vacher et al. 2020). However, the state of knowledge about the reptiles of this region is still incipient, especially regarding the relationships among the species and the complexity of

ecosystems in the region (Ávila-Pires et al. 2007; Morato et al. 2018). Thus, this study reinforces the importance of conservation units (even those of sustainable use) on maintaining populations that are still unknown to science.

Conclusion

The conservativeness of the external morphological characters of scolecophidians represent a challenge when trying to understand their evolution. Therefore, the combination of morphological (external and internal) and molecular data appears to be crucial in resolving systematic issues within this group. These data also reinforce the utility of osteological and hemipenial data in recognizing new taxa, especially amongst threadsnakes (Leptotyphlopidae). Even though scolecophidians are known for displaying a very conserved external morphology, polymorphic taxa—although rare—might still be unknown to science, therefore representing a true paradigm in the evolution of threadsnakes. Therefore, external morphological data might not be disregarded when considering the phenotypic evolution of the group and may as well be significant in identifying new taxa, including those that exhibit many autapomorphies.

Acknowledgements

We are thankful to the following persons for allowing us to examine specimens under their care: A.L.C. Prudente (MPEG); A. Resetar (FMNH); F. Grazziotin and G. Puerto (IBSP); F.L. Franco, F.F. Curcio (UFMT), G. Colli and M. Zatz (CHUNB), H. Zaher (MZUSP), J. Rosado (MCZ), K. de Queiroz, N. Camacho (LACM); N. Vidal (MNHN), O. Torres-Carvajal (QCAZ), R. Wilson, R. McDiarmid and A. Wynn (USNM); M. Pires (LZV/UFOP), R. Feio (MZUFV), R. Brown (KU). We thank F. Grazziotin for providing tissue samples of *Trilepida dimidiata*. A. Martins thanks Dr. Marcelo Soares for support with X-ray images at the Museu Nacional/UFRJ. We are thankful to Coordenação de Aperfeiçoamento de Pessoal de Nível Superior (Capes), to Conselho Nacional de Desenvolvimento Científico e Tecnológico (CNPq), to Fundação de Apoio a Pesquisa do Distrito Federal (FAPDF), and Fundação Carlos Chagas Filho de Amparo à Pesquisa do Estado do Rio de Janeiro (FAPERJ). We thank COMIP/IBAMA and Mineração do Rio do Norte (MRN) for allowing us to examine the specimens collected. We also thank staff from Reserve Naturelle de la Trinité. We warmly thank Thibaud Decaens and Emmanuel Lapied who collected the specimen from Mitaraka when digging for fossorial fauna. This specimen was collected during the “Our Planet Reviewed” Guyane-2015 expedition in the Mitaraka range, in the core area of the French Guiana Amazonian Park, organized by the MNHN and Pro-Natura international. The expedition was funded by the European Regional Development Fund (ERDF), the Conseil régional de Guyane, the Conseil général de Guyane, the Direction de l’Environnement, de l’Aménagement et du Logement and by the Ministère de l’Éducation nationale, de l’Enseignement supérieur et de la Recherche. It was realized in collaboration with the Parc Amazonien de Guyane. We also acknowledge support from an ‘Investissement d’Avenir’ grant managed by Agence nationale de la Recherche (CEBA, ref. ANR-10-LAB× -25-01). We are grateful for the comments from two anonymous reviewers for scrupulous revision of this manuscript.

References

- Adalsteinsson SA, Branch WR, Trape S, Vitt LJ, Hedges SB (2009) Molecular phylogeny, classification, and biogeography of snakes of the family Leptotyphlopidae (Reptilia, Squamata). *Zootaxa* 2244: 1–50.
- Akaike H (1974) A new look at the statistical model identification. *IEEE Transactions on Automatic Control* 19: 716–723. <https://doi.org/10.1109/TAC.1974.1100705>
- Altschul SF, Madden TL, Schaffer AA, Zhang J, Zhang Z, Miller W, Lipman DJ (1997) Gapped BLAST and PSI-BLAST: A new generation of protein database search programs. *Nucleic Acids Research* 25: 3389–3402. <https://doi.org/10.1093/nar/25.17.3389>
- Ávila-Pires TCS, Hoogmoed MS, Vitt LJ (2007) Herpetofauna da Amazônia. In: Nascimento LB, Oliveira ME (Eds) *Herpetologia no Brasil II*. Sociedade Brasileira de Herpetologia, Belo Horizonte, 14–28.
- Bell C, Daza J, Stanley E, Laver R (2021) Unveiling the elusive: X-rays bring scolecophidian snakes out of the dark. *The Anatomical Record* 304: 2110–2117. <https://doi.org/10.1002/ar.24729>
- Bickford D, Lohman, Sodhi N, Ng P, Meier R, Winker K, Ingram K, Das I (2006) Cryptic species as a window on diversity conservation. *Trends in Ecology and Evolution* 22: 148–155.
- Branch WR (1986) Hemipenial morphology of African snakes: A taxonomic review. Part 1. Scolecophidia and Boidae. *Journal of Herpetology* 20: 285–299.
- Broadley DG, Wallach V (2007) A revision of the genus *Leptotyphlops* in northeastern Africa and southwestern Arabia (Serpentes: Leptotyphlopidae). *Zootaxa* 1408: 1–78.
- Buser TJ, Boyd OF, Cortés A, Donatelli CM, Kolmann MA, Luparell JL, Pfeiffenberger JA, Sidlauskas BL, Summers AP (2020) The natural historian's guide to the CT galaxy: Step-by-step instructions for preparing and analysing computed tomographic (CT) data using cross-platform, open access software. *Integrative Organismal Biology* 2020: 1–25. <https://doi.org/10.1093/iob/obaa009>
- Cundall D, Irish F (2008) The snake skull. In: Gans C, Gaunt AS, Adler K (Eds) *Biology of the Reptilia*, Vol. 20, Morphology H. Society for the Study of Amphibians and Reptiles, New York: 349–692.
- De Queiroz K (2007) Species concepts and species delimitation. *Systematic Biology* 56: 879–886.
- Deolindo V, Koch C, Joshi M, Martins A (2021) To move or not to move? Skull and lower jaw morphology of the blindsnake *Afrotyphlops punctatus* (Leach, 1819) (Serpentes, Typhlopoidea, Typhlopidae) with comments on its previously advocated cranial kinesis. *The Anatomical Record* 304: 2279–2291. <https://doi.org/10.1002/ar.24598>
- Dewynter M, Courtois E, Massary JC de, Uriot Q, Uriot S, Prémel V, Villette B, Ruffray V, Perrier M, Bouchet L, Le Pape T, Foxonet H, Remérand E, Baudain D, Baglan A, Marty C, Bonnefond A (2020): La base de données Faune-Guyane (Amphibiens, Squamates, Tortues & Caïmans): Synthèse 2020. *Herp me!* 4: 1–87.
- Dowling HG, Savage JM (1960) A guide to the snake hemipenis: A survey of basic structure and systematic characteristics. *Zoologica* 45: 17–28.
- Ferreira AC, Klaczko J, Martins AR (2021) Hemipenial morphology of *Epictia vellardi* (Laurent, 1984) (Leptotyphlopidae, Serpentes) with the proposition and discussion of two general hemipenial patterns within the genus *Epictia*. *Zoomorphology* 140: 143–150. <https://doi.org/10.1007/s00435-020-00506-0>
- Francisco BC, Pinto RP, Fernandes DS (2012) Taxonomy of *Epictia mu-noai* (Orejas-Miranda, 1961) (Squamata: Serpentes: Leptotyphlopidae). *Zootaxa* 3512: 42–52.
- Francisco BC, Pinto RR, Fernandes D (2018) Taxonomic notes on the genus *Siagonodon* Peters, 1881, with a report on morphological variation in *Siagonodon cupinensis* (Bailey and Cervalho, 1946) (Serpentes, Leptotyphlopidae). *Copeia* 2018: 321–328. <https://doi.org/10.1643/CH-17-641>
- Graboski R, Arredondo J, Grazziotin F, Silva AA, Prudente ALC, Rodrigues MT, Bonatto S, Zaher H (2018) Molecular phylogeny and hemipenial diversity of South American species of *Amerotyphlops* (Typhlopidae, Scolecophidia). *Zoologica Scripta* 48: 139–156. <https://doi.org/10.1111/zsc.12334>
- Graboski R, Arredondo J, Grazziotin F, Guerra-Fuentes RA, Silva AA, Prudente ALC, Pinto RR, Rodrigues MT, Bonatto S, Zaher H (2022) Revealing the cryptic diversity of the widespread and poorly known South American blind snake genus *Amerotyphlops* (Typhlopidae: Scolecophidia) through integrative taxonomy. *Zoological Journal of the Linnean Society* 197: 1–33. <https://doi.org/10.1093/zoolinnean/zlac059>
- Grazziotin FG, Zaher H, Murphy RW, Scrocchi G, Benavides MA, Zhang YP, Bonatto SL (2012) Molecular phylogeny of the New World Dipsadidae (Serpentes: Colubroidea): A reappraisal. *Cladistics* 28: 437–459. <https://doi.org/10.1111/j.1096-0031.2012.00393.x>
- Hedges SB (2011) The type species of the threadsnake genus *Tricheilostoma* Jan revisited (Squamata, Leptotyphlopidae). *Zootaxa* 3027: 63–64.
- Hollowell T, Reynolds RP (2005) Checklist of the Terrestrial Vertebrates of the Guiana Shield. *Bulletin of the Biological Society of Washington* 13: 1–98.
- Holman JA (2000) Fossil snakes of North America: Origin, evolution, distribution, paleoecology. Indiana University Press, Bloomington, IN, 386 pp.
- Katoh K, Misawa K, Kuma K, Miyata T (2002) MAFFT: A novel method for rapid multiple sequence alignment based on fast Fourier transform. *Nucleic Acids Research* 30: 3059–3066. <https://doi.org/10.1093/nar/gkf436>
- Koch C, Martins AR, Schweiger S (2019) A century of waiting: Description of a new *Epictia* Gray, 1845 (Serpentes: Leptotyphlopidae) based on specimens housed for more than 100 in the collection of the Natural History Museum Vienna (NMW). *PeerJ* 7: e7411. <https://doi.org/10.7717/peerj.7411>
- Koch C, Martins AR, Joshi M, Pinto RR, Passos P (2021) Osteology of the enigmatic threadsnake species *Epictia unicolor* and *Trilepida guayaquilensis* (Serpentes: Leptotyphlopidae) with generic insights. *The Anatomical Record* 304: 2183–2197. <https://doi.org/10.1002/ar.24676>
- Laver R, Daza J (2021) Blind snakes beneath the surface: Continuing the legacy of Richard Thomas. *The Anatomical Record* 304: 2080–2084. <https://doi.org/10.1002/ar.247442084>
- Laver RJ, Daza J, Ellis R, Stanley E, Bauer A (2021) Underground down under: Skull anatomy of the southern blind snake *Anilius australis* Gray, 1845 (Typhlopidae: Serpentes: Squamata). *The Anatomical Record* 304: 1–28. <https://doi.org/10.1002/ar.246962242>
- Lira I, Martins AR (2021) Digging into blindsnakes' morphology: Description of the skull, lower jaw, and cervical vertebrae of two *Amerotyphlops* (Hedges et al., 2014) (Serpentes, Typhlopidae) with comments on the typhlopoidean skull morphological diversity. *The Anatomical Record* 304: 2198–2214. <https://doi.org/10.1002/ar.24591>
- List JC (1966) Comparative osteology of the snake families Typhlopidae and Leptotyphlopidae. *Illinois Biological Monographs* 36: 1–112.

- Marin J, Donnellan SC, Hedges SB, Puillandre N, Aplin K, Doughty P, Vidal N (2013) Hidden species diversity of Australian burrowing snakes (*Ramphotyphlops*). *Biological Journal of the Linnean Society* 110: 427–441. <https://doi.org/10.1111/bij.12132>
- Markolf M, Brameier M, Kappeler, PM (2011) On species delimitation: Yet another lemur species or just genetic variation? *BMC Evolutionary Biology* 11: 21. <https://doi.org/10.1186/1471-2148-11-21>
- Martins AR (2016) Morfologia Interna Comparada de Representantes da Subfamília Epictinae (Serpentes, Scolecophidia, Leptotyphlopidae). PhD Thesis, Museu Nacional/Universidade Federal do Rio de Janeiro, Rio de Janeiro.
- Martins AR, Passos P, Pinto R (2018) Unveiling diversity under the skin: Comparative morphology study of the cephalic glands in threadsnakes (Serpentes: Leptotyphlopidae: Epictinae). *Zoomorphology* 137: 433–443. <https://doi.org/10.1007/s00435-018-0409-8>
- Martins AR, Koch C, Pinto R, Folly M, Fouquet A, Passos P (2019a) From the inside out: Discovery of a new genus of threadsnakes based on anatomical and molecular data, with discussion of the leptotyphlopoid hemipenial morphology. *Journal of Zoological Systematics and Evolutionary Research* 57: 840–863. <https://doi.org/10.1111/jzs.12316>
- Martins AR, Passos P, Pinto R (2019b) Moving beyond the surface: Comparative head and neck myology of threadsnakes (Epictinae, Leptotyphlopidae, Serpentes), with comments on the ‘scolecochidial’ muscular system. *PLoS One* 14: e0219661. <https://doi.org/10.1371/journal.pone.0219661>
- Martins AR, Koch C, Joshi M., Pinto R, Passos P (2021a) Picking up the threads: Comparative osteology and associated cartilaginous elements for members of the genus *Trilepida* Hedges, 2011 (Serpentes, Leptotyphlopidae) with new insights on the Epictinae systematics. *The Anatomical Record* 304: 2149–2182. <https://doi.org/10.1002/ar.24747>
- Martins AR, Koch C, Joshi M, Pinto RR, Passos P (2021b) Picking up the threads: Comparative osteology and associated cartilaginous elements for members of the genus Hedges, 2011 (Serpentes, Leptotyphlopidae) with new insights on the Epictinae systematics. *The Anatomical Record* 304: 2149–2182. <https://doi.org/10.1002/ar.24747>
- Matioli SR, Fernandes FMC (2012) *Biologia molecular e evolução*. Ho-los, Ribeirão Preto, 256 pp.
- McCranie J, Hedges SB (2016) Molecular phylogeny and taxonomy of the *Epictia goudotii* species complex (Serpentes: Leptotyphlopidae: Epictinae) in Middle America and northern South America. *PeerJ* 4: e1551. <https://doi.org/10.7717/peerj.1551>
- Miller MA, Pfeiffer W, Schwartz T (2010) Creating the CIPRES Science Gateway for inference of large phylogenetic trees. In: *Proceedings of the Gateway Computing Environments Workshop (GCE)*, November 2010. New Orleans, LA. <https://doi.org/10.1109/GCE.2010.5676129>
- Miralles A, Marin J, Markus D, Herrel A, Hedges SB, Vidal N (2018) Molecular evidence for the paraphyly of Scolecophidia and its evolutionary implications. *Journal of Evolutionary Biology* 31: 1782–1793. <https://doi.org/10.1111/jeb.13373>
- Morato SAA, Ferreira GN, Scupino MRC (2018) Herpetofauna da Amazônia Central: Estudos na FLONA de Saracá-Taquera. STCP Engenharia de Projetos Ltda. and MRN – Mineração Rio do Norte S.A., Curitiba and Porto Trombetas, vii + 210 pp.
- Myers CW, Campbell JA (1981) A new genus and species of colubrid snake from the Sierra Madre del Sur of Guerrero, Mexico. *American Museum Novitates* 2708: 1–20.
- Orejas-Miranda BR (1967) El genero “*Leptotyphlops*” en la región Amazónica. *Atas do Simpósio sobre a Biota Amazonica* 5: 421–442.
- Passos P, Caramaschi U, Pinto R (2005) Rediscovery and redescription of *Leptotyphlops salgueiroi* Amaral, 1954 (Squamata, Serpentes, Leptotyphlopidae). *Boletim do Museu Nacional* 520: 1–10.
- Passos P, Caramaschi U, Pinto R (2006) Redescription of *Leptotyphlops koppesi* Amaral, 1954, and description of a new species of the *Leptotyphlops dulcis* group from Central Brazil (Serpentes: Leptotyphlopidae). *Amphibia–Reptilia* 27: 347–357.
- Pesantes OS (1994) A method for preparing the hemipenis of preserved snakes. *Journal of Herpetology* 28: 93–95.
- Peters JA (1970) Catalogue of the Neotropical Squamata: Part 1. Snakes. *Bulletin of the United States National Museum* 297: 1–347.
- Peters JA, Orejas-Miranda BR (1970) Notes on the hemipenis of several taxa in the family Leptotyphlopidae. *Herpetologica* 26: 320–324.
- Peters WCH (1881) Einige herpetologische Mittheilungen. *Sitzungsberichte der Gesellschaft naturforschender Freunde zu Berlin* 1881: 69–72.
- Pinto RR (2010) Revisão sistemática da Subtribo Renina (Serpentes: Leptotyphlopidae) PhD Thesis, Museu Nacional /Universidade Federal do Rio de Janeiro, Rio de Janeiro.
- Pinto R, Passos P, Portilla J, Arredondo J, Fernandes R (2010) Taxonomy of the threadsnakes of the tribe Epictini (Squamata: Serpentes: Leptotyphlopidae) in Colombia. *Zootaxa* 2724: 1–28.
- Pinto RR, Curcio F (2011) On the generic identity of *Siagonodon brasiliensis*, with the description of a new leptotyphlopoid from central Brazil (Serpentes: Leptotyphlopidae). *Copeia* 2011: 53–63.
- Pinto RR, Fernandes R (2012) A new blind snake species of the genus *Tricheilostoma* from Espinhaço range, Brazil and taxonomic status of *Rena dimidiata* (Jan, 1861) (Serpentes: Epictinae: Leptotyphlopidae). *Copeia* 2012: 37–48.
- Pinto R, Fernandes R (2017) Morphological variation of *Trilepida macrolepis* (Peters 1857), with reappraisal of the taxonomic status of *Rena affinis* (Boulenger 1884) (Serpentes: Leptotyphlopidae: Epictinae). *Zootaxa* 4244: 246–260. <https://doi.org/10.11646/zootaxa.4244.2.6>
- Posada D (2008) jModelTest: Phylogenetic model averaging. *Molecular Biology and Evolution* 25: 1253–1256. <https://doi.org/10.1093/molbev/msn083>
- Rambaut A, Drummond AJ (2007) Tracer, version 1.4. Retrieved from Archived by WebCite at: <http://beast.bio.ed.ac.uk/tracer>
- Rieppel O, Kley NJ, Maisano JA (2009) Morphology of the skull of the white-nosed blindsnake, *Liotyphlops albirostris* (Scolecophidia: Anomalepididae). *Journal of Morphology* 270: 536–557. <https://doi.org/10.1002/jmor.10703>
- Ronquist F, Huelsenbeck P (2003) MrBayes: Bayesian phylogenetic inference under mixed models. *Bioinformatics* 19: 1572–1574.
- Salazar-Valenzuela D, Martins AR, Amador-Oyola L, Torres-Carvajal O (2015) A new species and country record of threadsnakes (Serpentes: Leptotyphlopidae: Epictinae) from northern Ecuador. *Amphibian and Reptile Conservation* 8: 107–120.
- Santos FJM, Reis RE (2018) Two new blind snake species of the genus *Liotyphlops* (Serpentes: Anomalepididae), from Central and South Brazil. *Copeia* 2018: 507–514. <https://doi.org/10.1643/CH-18-81>
- Santos FJM, Reis R (2019) Redescription of the blind snake *Anomalepis colombia* (Serpentes: Anomalepididae) using high-resolution X-ray computed tomography. *Copeia* 2019: 239–243. <https://doi.org/10.1643/CH-19-181>
- Silva JMC, Garda, AA (2010) Padrões e processos biogeográficos na Amazônia. In: Carvalho CJB, Almeida EAB (Eds) *Biogeografia da*

- América do Sul: Padrões e Processos. Ed. São Paulo, São Paulo, 189–197.
- Struck T, Feder J, Bendiksbj M, Birkeland S, Cerca J, Gusarov V, Kistenich S, Larsson K, Liow L, Nowak M, Stedje B, Bachman L, Dimitrov D (2018) Finding evolutionary processes hidden in cryptic species. *Trends in Ecology & Evolution* 33: 153–163. <https://doi.org/10.1016/j.tree.2017.11.007>
- Townsend TM, Alegre RE, Kelley ST, Wiens J, Reeder T (2008) Rapid development of multiple nuclear loci for phylogenetic analysis using genomic resources: An example from squamate reptiles. *Molecular Phylogenetics and Evolution* 47: 129–142. <https://doi.org/10.1016/j.ympev.2008.01.008>
- Uetz P, Freed P, Hosek J (2022) The reptile database. Electronic Database accessible at <http://www.reptile-database.org>. Accessed on 11 November 2022.
- Vacher JP, Chave J, Ficetola FG, Sommeria-Klein G, Tao S, Thebaud C, Blanc M, Camacho A, Cassimiro J, Colston T, Dewynter M, Ernst R, Gaucher P, Gomes J, Jairam R, Kok P, Lima J, Martines Q, Marty C, Noonan B, Nunes P, Recoder R, Rodrigues M, Snyder A, Marques-Souza S, Fouquet A (2020) Large-scale DNA-based survey of frogs in Amazonia suggests a vast underestimation of species richness and endemism. *Journal of Biogeography* 47: 1781–1791. <https://doi.org/10.1111/jbi.13847>
- Wallach V (2016) Morphological review and taxonomic status of the *Epictia phenops* species group of Mesoamerica, with description of six new species and discussion of South American *Epictia albifrons*, *E. goudotii*, and *E. tenella* (Serpentes: Leptotyphlopidae; Epictiinae). *Mesoamerican Herpetology* 3: 216–374.
- Vidal N, Hedges SB (2005) The phylogeny of squamate reptiles (lizards, snakes, and amphisbaenians) inferred from nine nuclear protein-coding genes. *Comptes Rendus Biologies* 328: 1000–1008. <https://doi.org/10.1016/j.crvi.2005.10.001>
- Vidal N, Marin J, Morini M, Donnellan S, Branch WR, Thomas R, Vences M, Wynn A, Cruaud C, Hedges SB (2010) Blindsnake evolutionary tree reveals long history on Gondwana. *Biology Letters* 6: 558–561. <https://doi.org/10.1098/rsbl.2010.0220>
- Zaher H, Grazziotin FG, Cadle J, Murphy R, Moura-Leite JC, Bonatto S (2009) Molecular phylogeny of advanced snakes (Serpentes, Caenophidia) with an emphasis on South American Xenodontines: A revised classification and descriptions of new taxa. *Papéis Avulsos de Zoologia* 49: 115–153.

Appendix 1

* Specimens with one asterisk were μ CT-scanned for skull comparisons.

** Specimens with double asterisk were analyzed based on dry or cleared and stained specimens

- Epictia ater*. **EL SALVADOR**: San Miguel: KU 183846**; NICARAGUA: CHINANDEGA: Volcan Chongo: KU 194336, 200596; ESTELLI: KU 174119, 174120–21, 174134–35.
- Epictia goudotii*. **VENEZUELA**: Aragua: Girardot: Cuyagua: USNM 258148*.
- Epictia magnamaculata*. **HONDURAS**: Islas de la Bahía: Isla de Utila: USNM 54760.
- Epictia munoai*. **URUGUAY**: Tacuarembó: Tambores: Pozo Hondo: USNM 163506.
- Epictia phenops*. **MEXICO**: Yucatán: FMNH 20606**, 36345**, OAXACA: FMNH 111477**, 111481; QUINTANA ROO: Isla Cozumel: LACM 127814**.
- Epictia rufidorsa*. **PERU**: Lima: Rimac Valley: USNM 49993.
- Epictia tenella*. **BRAZIL**: AMAZONAS: Urucá: MNRJ 18831; PARÁ: Oriximiná: Porto Trombetas: MNRJ 16827*, 16828*; TRINIDAD AND TOBAGO: TRINIDAD: Arima: USNM 536525*; Guayaquayare: MCZ 60801; Mathura: MCZ 96538–39; Mazanilla Beach: MCZ 160087*; Parrylands: MCZ 160088; Port of Spain City Corporation: MCZ 79785–86; San Juan-Laventille Regional Corporation: MCZ 28208; Trinity Hills: MCZ 38660.
- Habrophallos collaris*. **FRENCH GUIANA**: Itoupe: MNHN 2019.0002–3; No locality: MNHN 1977.49*, MNHN 1996.4580*; Nouragues Pararé: MNRJ 27144; Saül: MNHN 1999.8309*; Saul Limonade: MNHN 2019.0001; Trinité: MNRJ 27145; SURINAME: Brownsberg: AF 3912.
- Siagonodon cupinensis*. **BRAZIL**: Mato Grosso: Barra do Tapirapes: MNRJ 387 (holotype), MZUSP 4405; Guaranta do Norte: UFMT 4261–62, 4476, 5572, 5574–75, 5578 5580, 5582, 5587–88, 5591–92, 5594, 5596–97, 5602, 5604, 5606, 5608, 5611–12, 5618, 5620, 5622–4, 5626, 5627*, 5629, 5631–32, 5635–39, 5644, 5646–47, 5649, 5651–55, 5657–59, 5661–2, 5664, 5667, 5672, 5675, 6372, 6374, 6378–80.
- Siagonodon exiguum*. **BRAZIL**: Pará: Monte Branco, Oriximiná: MNRJ 27557–6 (paratypes), MNRJ 27562* (holotype). **FRENCH GUIANA**: Maripasoula: Mitaraka: MNHN-RA 2023.0001* (paratype).
- Siagonodon septemstriatus*. **BRAZIL**: Amazonas: Manaus: Negro River: Negro Rover Bank (NMW 15476/1); Presidente Figueiredo: IBSP 51897*. **SURINAME**: without locality (ZSM 127/1947, ZMB 3876, holotype).
- Trilepida acutirostris*. **BRAZIL**: Tocantins: Almas: CHUNB 35648 (holotype); Mateiros: CHUNB 41097 (paratype*).
- Trilepida brasiliensis*. **BRAZIL**: Mato Grosso do Sul: Corumbá (UFMT 683, 1159**, 1160, 1162–63**, 1169); Rosário d'Oeste (MNRJ 24334*).
- Trilepida dimidiata*. **BRAZIL**: Roraima: Boa Vista (MZUSP 10090**, 10120*), Ilha de Maracá: (BMNH 1994.241).
- Trilepida fuliginosa*. **BRAZIL**: Goiás: Caldas Novas (MZUSP 11111); Colinas do Sul (MNRJ 19223); Luziânia (MNRJ 10034, holotype), CHUNB 40788, 40847**, 408486); Minaçu (MZUSP 11019); Ouidor (MNRJ 19221); Minas Gerais: Unaí (MNRJ 24400); Tocantins: Porto Alegre do Tocantins (CHUNB 38928).
- Trilepida jani*. **BRAZIL**: Minas Gerais: Ouro Preto (LZV 813S**); Ouro Branco (LZV 778S*); without locality (MNRJ 16990).
- Trilepida joshuai*. **COLOMBIA**: Antioquia: Jericó (IBSP 8919*); Valle del Cauca: Tocota: (NMW 38424/1–2).
- Trilepida koppesi*. **BRAZIL**: Aporé (MNRJ 24715**–16*); Mineiros (CHUNB 25714**, 40788**); Mato Grosso do Sul: Terenos: (IBSP 8883, holotype).
- Trilepida macrolepis*. **BRAZIL**: Pará: Paraupébas: Floresta Nacional de Carajás (MPEG 23017*); **COLOMBIA**: Vale del Cauca: Buenaventura (USNM 154031, 267261); Córdoba: Pueblo Nuevo (ICN 7677); **ECUADOR**: Esmeraldas: Durango (QCAZ 12494*); **VENEZUELA**: Mérida (NMW 15468/1–4); Yaracuy: Salom (MTKD 26320–21).
- Trilepida pastusa*. **ECUADOR**: Carchi: Tulcán (QCAZ 5778*).
- Trilepida salgueiroi*. **BRAZIL**: Bahia: São José do Macuco (currently São José da Vitória) (MZUSP 9098); Espírito Santo: Governador Lindemberg (MNRJ 12131–32); “Itá” currently Baixo Guandu: (IBSP 8876, holotype); Aracruz (MNRJ 4856**); Campinho (MNRJ 1925); Linhares, Goytacazes (MNRJ 1926), Sooretama (MZUSP 2463); Minas Gerais: Aimorés (MCNR 1468-1469, MNRJ 12239), Muriaé: (MZUFV 1519); Recreio (MNRJ 7856); Rio de Janeiro: Cambuci (MNRJ 14487**); Niterói: Itaipu (MNRJ 13124, 15422**).

Supplementary Material 1

Table S1

Authors: Martins A, Folly M, Ferreira GN, Garcia da Silva AS, Koch C, Fouquet A, Machado A, Lopes RT, Pinto R, Rodrigues MT, Passos P (2023)

Data type: .xlsx

Explanation note: GenBank accession number for specimens used in the current study.

Copyright notice: This dataset is made available under the Open Database License (<http://opendatacommons.org/licenses/odbl/1.0>). The Open Database License (ODbL) is a license agreement intended to allow users to freely share, modify, and use this Dataset while maintaining this same freedom for others, provided that the original source and author(s) are credited.

Link: <https://doi.org/vz.73.e98170.suppl1>

Supplementary Material 2

Table S2

Authors: Martins A, Folly M, Ferreira GN, Garcia da Silva AS, Koch C, Fouquet A, Machado A, Lopes RT, Pinto R, Rodrigues MT, Passos P (2023)

Data type: .xlsx

Explanation note: Genetic distances of *Siagonodon* spp. in comparison to other Epictinae genera based on 16s sequences.

Copyright notice: This dataset is made available under the Open Database License (<http://opendatacommons.org/licenses/odbl/1.0>). The Open Database License (ODbL) is a license agreement intended to allow users to freely share, modify, and use this Dataset while maintaining this same freedom for others, provided that the original source and author(s) are credited.

Link: <https://doi.org/vz.73.e98170.suppl2>

Supplementary Material 3

X-Ray Images

Authors: Martins A, Folly M, Ferreira GN, Garcia da Silva AS, Koch C, Fouquet A, Machado A, Lopes RT, Pinto R, Rodrigues MT, Passos P (2023)

Data type: .zip

Explanation note: X-Ray Images of specimens of *Siagonodon exiguum* sp. nov.

Copyright notice: This dataset is made available under the Open Database License (<http://opendatacommons.org/licenses/odbl/1.0>). The Open Database License (ODbL) is a license agreement intended to allow users to freely share, modify, and use this Dataset while maintaining this same freedom for others, provided that the original source and author(s) are credited.

Link: <https://doi.org/vz.73.e98170.suppl3>